

Secondary Electron Emission Studies of Lithiated Diamond Exposed to Beta Radiation

Rabi Emran

(Dayangku Rabiatul Adawiyah Iylia Pengiran Haji Emran)

2013

Dissertation submitted in accordance to obtaining a BSc in
Chemistry.

Supervisor: Dr. Neil Fox

Second Assessor: Prof. Paul May



University of
BRISTOL

Acknowledgement

First and foremost, I would like to express my deepest appreciation to my supervisor; Dr. Neil Fox for his guidance and persistence help in this project. I would also like to thank my second supervisor, Prof Paul May for his valuable help. I also thank Dr. James Smith for being extremely helpful since day one of my lab work. The technical support he has provided will always be appreciated.

My sincere thanks go to Liam Payne from the Interface Analysis Centre for his supervision and providing me with all the necessary facilities. And also a massive thanks to Jan Harwood from Physics for setting up the "Jan Machine" that saved my life.

I would also like to take this opportunity to thank the BUDGies (Bristol University Diamond Group) for their help and encouragement, especially Sarah Halliwell, James King, Dr. Oliver Fox and Hugo Dominguez for helping me with my sample preparation. I am indebted to Vijay Chatterjee for giving his time in assisting me with the secondary electron emission yield measurement –without him my experimental work would have not developed.

Additionally, I extend my thanks to Dr. Richard Schubert-Rowles from KRÜSS Surface Science Centre in the School of Chemistry for his technical consultation on the contact angle measurement.

Special mention goes to Zamir Othman who has inspired me greatly to get me through this project. Without his help and motivation, this dissertation would not have been possible. His enthusiastic encouragement and constructive feedback has helped me a lot throughout my final year.

Not to forget to mention, I am thankful for the undying support given by Richmonds, particularly Hani Yaakub from Geology Department for proof reading my work and also for being there for the last three years. Thank you!

And last but not least, I present this work especially for my Mummy&Babah.

Alhamdulillah.

Abstract

The formation of dipole layer on the surface terminations of diamond and the impurities incorporated in the bulk of diamond can result in the formation of negative electron affinity (NEA) effect on the surface. How NEA improved the secondary electron emission yield (δ), with respect to the presence of dipole, was discussed. Four different sample terminations have been prepared and both qualitative and quantitative secondary electron emission studies were carried out by secondary electron microscopy and Faraday cup measurement respectively. Hydrogen terminated has the highest secondary electron emission yield, followed by lithium-oxygen terminated, oxygen terminated and finally lithium fluoride-oxygen terminated sample having the lowest yield. The highest secondary yield obtained in this study appeared at primary beam energy, E_p of 0.6 keV with a yield of $\delta=5.88$ for H-termination, followed by $\delta = 3.86$ for Li-O-termination, $\delta=1.57$ for O-termination and $\delta=1.48$ for LiF-O-termination. The contact angles of the four different surface terminations were also determined to characterize the wetting properties.

Table of Contents

Abstract	3
Part 1: Introduction	
1.1 Diamond	7
1.1.1 High-pressure high-temperature synthesis (HPHT)	8
1.1.2 Chemical Vapor Deposition	8
1.1.3 Substrate	9
1.1.4 Type of diamond	9
1.1.5 Diamond surfaces	9
1.2 Theory	
1.2.1 Band diagram	11
1.2.2 Band bending	12
1.2.3 Electron affinity	13
1.2.4 Negative electron affinity	13
1.2.5 True and effective NEA	14
1.2.6 Work function	15
1.3 Semiconductors	16
1.3.1 Semiconductor properties	16
1.4 Secondary Electron Emission	17
1.4.1 Secondary Electron emission yield	19
1.5 CVD diamond films	20
1.5.1 Introduction of chemical dopants	20
1.5.2 Surface Treatments	21
1.5.3 Termination	22
1.5.4 Hydrogen terminated	23
1.5.5 Oxygen terminated	24
1.5.6 Thin films of metal	24
1.5.7 Alkali metal on oxygen terminated	25
1.6 Different types of primary beams	27

1.7 Aims and objectives	28
Part 2: Experimental	
2.1 Experimental method	29
2.1.1 Sample preparation	29
2.1.2 Sample characterization	30
2.1.3 Secondary electron emission studies	31
2.2 Introduction	33
2.2.1 Sample preparation	33
2.2.2 Cleaned samples	33
2.2.3 Ozone cleaner	33
2.2.4 H-termination	33
2.2.5 Lithiation	34
2.2.6 Li-F deposition	34
2.2.7 Sample characterization	34
2.2.8 Energy dispersive X-ray (EDX)	34
2.2.9 Contact angle measurement	35
2.2.10 Conductivity test	35
2.2.11 Secondary electron emission studies	35
2.2.12 Scanning electron microscope (SEM)	35
2.2.13 Secondary electron emission yield measurement	35
2.3 Results and discussion	37
2.3.1 Sample characterization	38
2.3.2 Energy dispersive X-ray (EDX)	38
2.3.3 Contact angle measurement	40
2.3.4 Conductivity test	41
2.3.5 Secondary electron emission studies	42
2.3.6 Scanning electron microscope (SEM)	42
2.3.7 Secondary electron emission (SEE) yield measurement	45
2.4 Conclusion	50

2.5 Further work	51
2.6 Appendices	52
2.6.1 EDX data	52
2.6.2 Contact angle data	54
2.6.3 SEM data	56
2.7 References	57

Part 1: Introduction

1.1 Diamond

Diamond is one of the materials that would be an ideal source of electrons, which can be promising for electron emission applications because carbon materials are generally thought of as having a low threshold towards ejecting electrons. Diamond has a four-fold coordinated structure comprising of just carbon and no other elements. Its four sets of sp^3 hybrid orbitals that are in a tetrahedral shape configuration differentiate it from the three-fold structure owned by the two other carbon allotropes; graphite and graphene. Being known as one of the materials that owns a large band gap, diamond, existing as an insulator with a band gap of 5.47eV ^[1] at 300 K, is a result of the good overlap of electron orbitals between adjacent carbon. Diamond is one of the hardest natural materials with a high thermal conductivity at room temperature. Diamond's inertness to most chemical reagents and its rigidity allow it to be transformed to thin films of a few microns thick that may be used in electronic applications. Diamond also previews a transparency in its optical properties, which makes it a brilliant gemstone. ^[2]

This form of allotrope of carbon is very expensive to exploit because the abundance of natural diamond in nature is lacking. Then it was found reacting carbon under very high pressure and high temperature condition can yield diamond commercially. This method was in fact a revolution of artificial diamond discovery. Efforts to synthesize diamond artificially started to become popular when the first synthetic method was modified with different variables to produce artificial diamond of extreme properties.

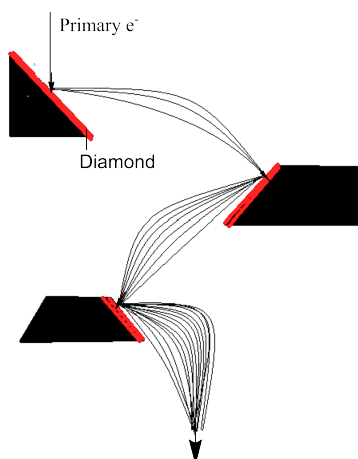


Figure 1.1: Diagram of a diamond-based photomultiplier tube in reflection mode Image adapted from^[3].

The diamond-based device of interest would be one that has a high secondary yield in which it can eject a large number of electrons, especially valuable for electron multiplication purposes like a photomultiplier tube for example. If diamond was to be coated on the stages of a photomultiplier tube as on figure 1.1, the incoming current will be amplified along the multiple stages forming a large current signal at the end of the tube that would be proportional to the incident

current. This would also mean diamond-based photomultiplier can be used as a sensor to detect a trace amount of beta radiation.

Metals and semi-conductors are generally poor at emitting secondary electrons unlike insulators. However insulators do not have the ability to replenish electrons lost during emission. Therefore doping of diamond can give the insulating diamond a semiconductor characteristic. Diamond, in its doped form, can exhibit an unusually high secondary electron yield so long as dopants can provide some level of electrical conductivity ^[4]. Attention has then been brought to alter the electronic properties of diamond so it can be transformed into an efficient electron source device.

1.1.1 High-pressure high-temperature synthesis (HPHT)

The earliest method used to produce diamond was by converting graphite using a metallic catalyst under high temperature and hydraulic pressure until the diamond crystallizes. ^[5] As a consequence to the low cost in carrying out this process, the resulting diamond would be in a very limited shape. Therefore due to this constraint, an alternative method called chemical vapor deposition (CVD) was discovered.

1.1.2 Chemical Vapor Deposition

Chemical vapor deposition (CVD) diamond is a synthetic diamond made using a chemical vapor deposition technique. The formation of thin film via gas-phase chemical reaction in a layer-by-layer technique imposed in this chemical process is used to produce very pure and high performance materials that can be implanted in semiconductors. Compared to HPHT method, CVD can function at a lower pressure and more importantly, at a lower cost of production. CVD can produce diamond with high thermal conductivities that can be utilized in microelectronics and optoelectronic applications such as in lasers and detectors. ^[6] Different types of CVD processes such as hot filament, microwave plasma, DC plasma, plasma jet, and arc discharge are based on the nature of growth conditions and activation processes. ^[6]

The common carbon-containing precursor molecules introduced into the gas source of CVD are CH₄ and H₂. The key reaction step of the growth process is the activation of these gases thermally by a hot filament or via the formation of plasma by microwave. The dissociated CH₄ and H₂ will be converted into reactive species. Collision of these reactive fragments with each other then occurs at high temperatures up to a few thousand kelvins until they touch the substrate surface. Once they get absorbed onto the active site of the substrate at the right orientation, nucleation process will occur resulting in the growth process of diamond. ^[6] Variation in the ratio of the gas source mixture in the activation region would usually be one of the ways to vary the composition and the orientation facets (100,111) of the diamond.

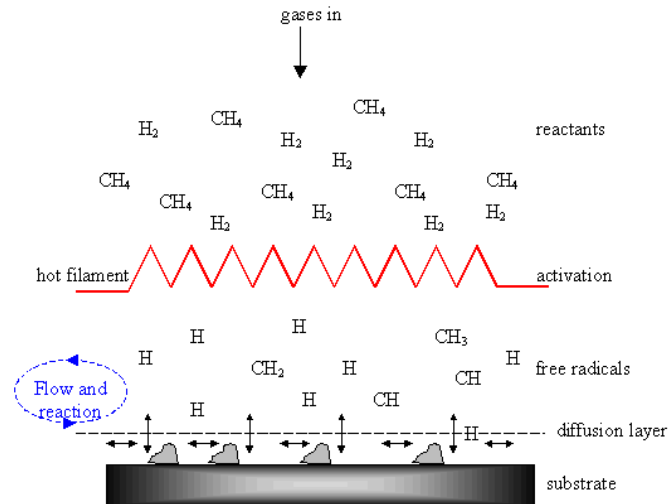


Figure 1.1.2: A simplified scheme of growing diamond in the CVD chamber. Gas reactants diffuse to the activation region to form reactive radicals that will get adsorbed on the substrate resulting in diamond growth. Image taken from [7]

1.1.3 Substrate

The material on which a diamond layer is deposited on during a CVD process is called the substrate. The requirements for the choice of substrate for CVD diamond are high melting point to allow the growth of diamond and similar thermal expansion to diamond to avoid physical deterioration of the sample film as temperature varies. Another important requirement a substrate needs to have is the ability to form a thin carbide layer with diamond, especially when diamond is grown to a non-diamond substrate. This thin carbide layer is essential as it adheres the synthesized diamond onto the surface of the substrate. [7]

1.1.4 Types of diamonds

Diamonds are classified into different types according to the quantity of impurities found within them. Type Ia diamond is described for impurities that are present as an aggregate or located on interstitial positions in the crystal lattice. [8] Type Ib has its impurities preferring the substitutional sites. It is called substitution because atom of an element other than carbon replaces the position of carbon atom lost in the lattice. As for diamond of type IIb, it is commonly doped with boron. Type IIb is the only single crystal that has impurities that are electronically active [9].

1.1.5 Diamond Surfaces

Within the lattice of diamond, there are three principle planes on the surface of a diamond. The three low index surface orientations of diamond are (100), (110) and (111). The (100) facet has two dangling bonds per surface atom while both (110) and (111) have only one dangling bond per surface atom. If the atoms on the dangling bonds of the diamond surface are changed, it can tune the electron affinity property of the surface, which will be covered later on in this paper.

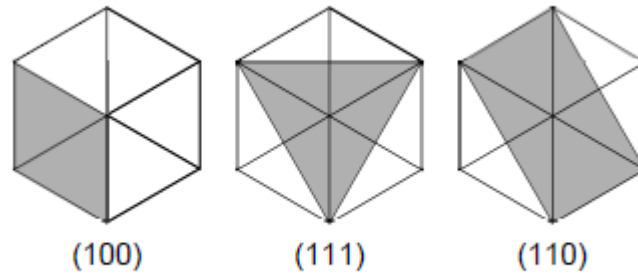


Figure 1.15: Planes of 100, 111 and 110 in an arbitrary unit cell. Image taken from [10]

1.2.1 Band diagram

Band diagram shows the band structure of the filled and unfilled orbital bands in relative to each other. The first approach to design the band structure of diamond was carried out by Painter, Ellis and Lubinsky using the Ab Initio method. [11] On the band diagram on figure 1.2.1.1, there is a valence band consisting of orbitals, which can be fully or partially filled with electrons. The gap between valence band maximum, $_{\max}E_v$ and conduction band minimum, $_{\min}E_c$ represents the band gap of a material. For semiconductors, conduction band generally appears above the valence band. Unless the electrons are excited, there will be no electrons found diffusing in the conduction band due to the band gap acting as a barrier. The value of conduction band minimum $_{\min}E_c$ of a material would be chosen with respect to the Fermi level, E_F , and has been determined by extrapolating the position of negative electron affinity peak to zero on the normal emission spectra of study made by Diederich group. [9] Electron affinity appears on the band structure as the difference between $_{\min}E_c$ and E_{vac} . It is considered as the energy acquired for an excited electron in the conduction band to overcome the barrier to emission out of the surface. Work function, Φ , is defined as the separation between the vacuum level E_{vac} and the Fermi level, E_f . Vacuum level, E_{vac} represents the energy level at which electrons are no longer bound to the surface of the material and so are free to be emitted into the vacuum. The value of E_{vac} was determined by the low-kinetic-energy cut-off of the XP normal emission spectra of a material. [9]

It should be worth noting that the energy distribution of internal electrons in the bulk is not the same as the energy distribution on the surface causing an effect called band bending. The presence of band bending demonstrates the differing position of the conduction band in the bulk compared to the position of the conduction band on the surface. This phenomenon is a result of the movement of electrons between the bulk and the surface. [12]

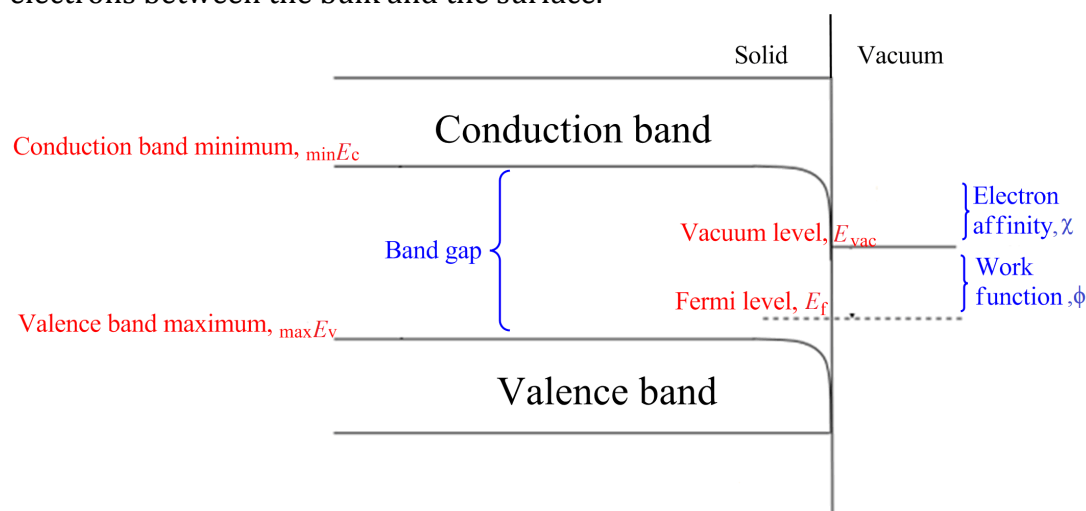


Figure 1.2.1.1: A band diagram of a p-type semi-conductor that has a negative electron affinity surface showing its E_{vac} lying below the $_{\min}E_c$. Image adapted from [13].

The band structures for semiconductors deviate depending on how the materials gain their semiconducting character. Band diagrams of the two different types of semiconductors; p-type and n-type are shown on figure 1.2.1.2. P-type semiconductors have their Fermi level; E_F appearing just above the valence band minimum and n-type semiconductors align its Fermi level, E_F just below the conduction band minimum. When electrons start to occupy the conduction band, with the vacuum level E_{vac} sitting anywhere below the whole conduction band, the electrons will have little or no barrier to emission and this effect displayed by the surface of a material is called negative electron affinity. If the vacuum level lies above the conduction band minimum on the band scheme, this acts as an energy barrier for electrons to leave the surface giving the material a positive electron affinity effect.

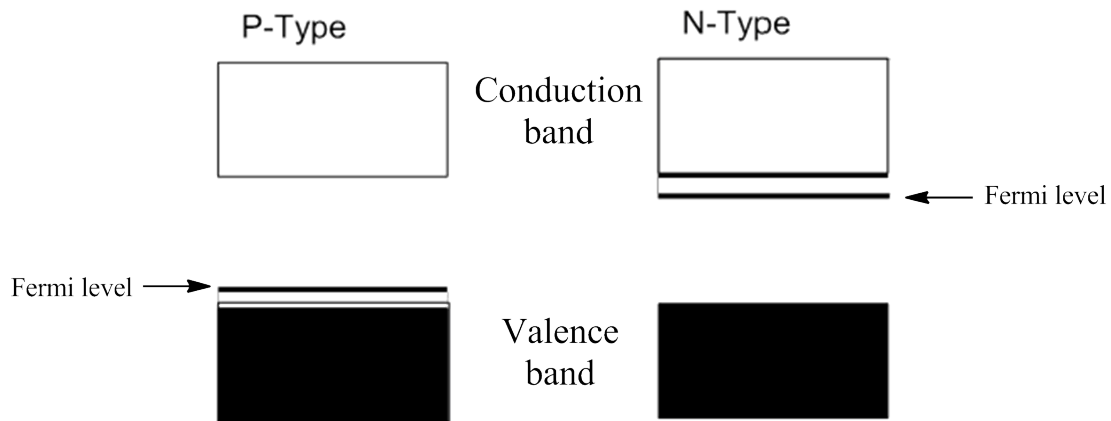


Figure 1.2.1.2: Diagram shows the relative positions of the Fermi level, E_F of a p-type semiconductor on the left and an n-type semiconductor. Image modified from [14].

1.2.2 Band bending

With a difference of E_F levels on the surface and in the bulk due to doping, charge carriers ie electrons can be transferred between the bulk and the surface. This movement of charge carriers justifies the type of bending on the surface energy band either upwards or downwards. N-type semiconductors usually have its energy band bending upwards due to the transfer of electrons from the bulk of a donor atom to the unoccupied surface state. Meanwhile, acceptor atoms in p-type materials do the reverse, in which they accept electrons from the surface states into their acceptor levels in the bulk showing a downward band bending as shown in figure 1.2.2. Band bending is rather regarded as a graphical representation for the difference in energy levels in the bulk and on the surface.

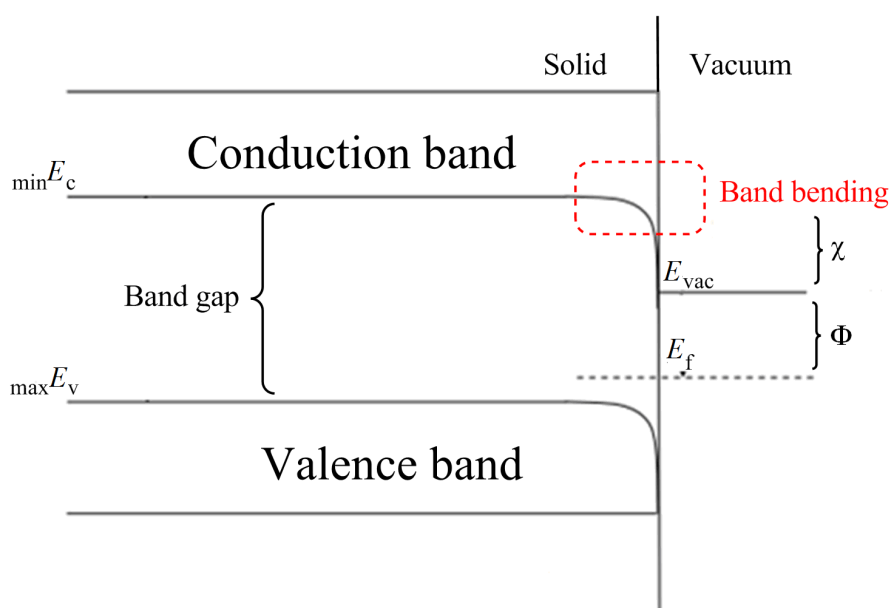


Figure 1.2.2: Red dotted region emphasizing the band bending on a band diagram.

1.2.3 Electron affinity

The definition of electron affinity is the energy change for the process of removing an electron from a singly charged negative ion. Referring to the band structure of any material, the electron affinity, χ , is the energy difference between the vacuum level E_{vac} and the lowest level of unoccupied electronic state i.e. conduction band minimum $min E_c$. This gap is the barrier that needs to be overcome by a low energy electron in a conduction band in order to escape into the vacuum. Insulators are known to be able to emit electrons efficiently, however they cannot supply conducting electrons that semi-conductors can to replenish the electrons lost from the surface. This is why semi-conductor makes a good electron-emitting device as it provides conducting electrons that can be thermalized from the valence band into the conduction band upon emission. ^[15]

1.2.4 Negative Electron Affinity (NEA)

The energetic barrier an electron needs to overcome preceding to emission, simply known as electron affinity, typically of a few eV ^[16], is the reason why excited electrons in the conduction band don't spontaneously leave the surface. A barrier is present when the vacuum level E_{vac} is situated above the conduction band; an effect called the positive electron affinity as portrayed on figure 1.2.5.1. Positive electron affinity usually limits the probability of electrons emitted to the vacuum, especially if the electrons in the bulk do not have sufficient energy to occupy E_{vac} . Therefore focus has been diverted to create a surface with a negative electron affinity, as this barrier is either reduced or omitted resulting in a spontaneous emission of a thermalized electron. ^[12]

A phenomenon when E_{vac} of a material lies under $\min E_c$ can be achieved via doping or surface terminations.^[17] In this case, when electrons start to occupy any of the conduction band states, they will escape out of the material readily because they have energy higher than the vacuum level and are no longer bound to the surface. Materials that can display negative electron affinity are desirable for electron emission applications.

1.2.5 True and Effective NEA

Research led by Mearini ^[18] found that negative electron affinity could be subdivided into two distinct types; the effective NEA and the true NEA. Generally both true and effective NEA have the same effect due to the position of vacuum level lying below the minimum conduction band; the only difference is, the effective NEA arises from the result of band bending at the surface. From the band diagram of an effective NEA surface on figure 1.2.5.2(b), it can be seen that the bulk minimum conduction is higher than E_{vac} , while the surface conduction minimum lies below it. Under the effective NEA condition, $\min E_c$ bend downwards to allow non-thermalized electrons to escape, resulting in low-energy secondary electrons ejected out. The extent of band bending in diamond can be controlled by doping and surface termination with metal coating. ^[19]

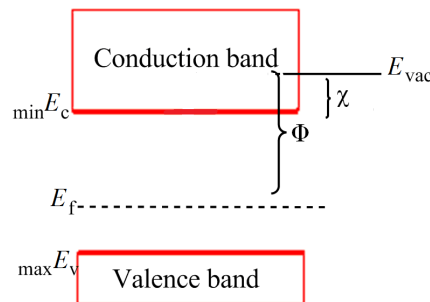


Figure 1.2.5.1: Energy band diagram of a positive electron affinity surface.

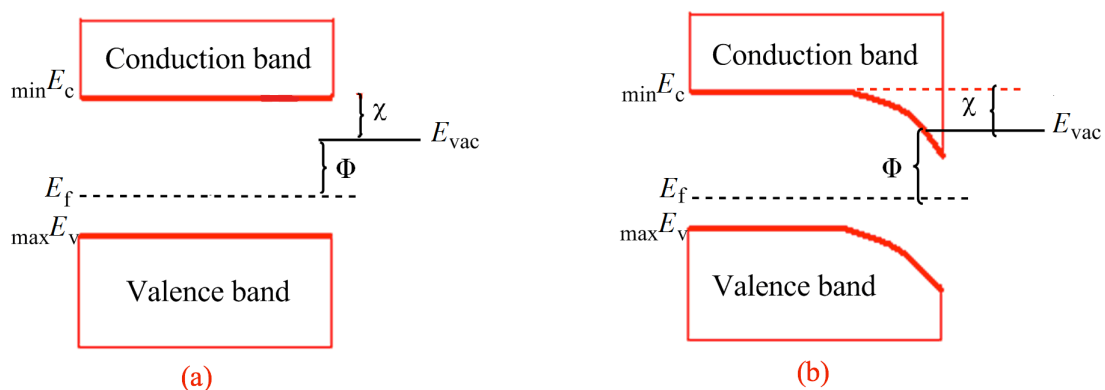


Figure 1.2.5.2: Surfaces that have E_{vac} lying below the conduction band showing a) a true negative electron affinity surface and b) an effective electron affinity surface.

1.2.6 Work function

Materials have a specific property called the work function, Φ , which is usually defined with respect to a hypothetical potential energy of an electron in a solid matched to the chemical potential which is known as the Fermi level, E_F . Work function is visualized as the energy required to move an electron from the Fermi level E_F to the vacuum level E_{vac} on the band diagram on figure 1.2.11. Therefore an alteration to the position of the Fermi level consequently varies the value of the work function. Studies made by Diederich^[9] proved the dependence of Fermi level and work function of a material to its surface morphology because there were different work function values of a diamond for C(100) (2x1):H and C(111) (1x1):H surfaces.^[14]

Adding dopants or reconstructing the surface of a material can alter the values of work function, which makes an important factor in predicting the spontaneity of electron emission. Factors that can lower the vacuum level E_{vac} of the surface below the conduction band minimum E_c , following a smaller gap between E_{vac} to the E_F not only creates an NEA effect but it also lowers the work function of a material (see figure 1.2.5.1 and 1.2.5.2). In short, work functions work hand in hand with the presence of NEA; therefore a reduced work function will allow a higher yield of secondary electrons emission as the surface barrier is reduced.

1.3 Semiconductors

Semiconductors with large band gap are good candidates for NEA applications for two reasons, firstly because the decay of excited electron can be prevented by the presence of the band gap and secondly because their conduction bands are more likely to be situated close to the vacuum level E_{vac} . However, too large of a band gap is only a characteristic of an insulator, which might not be able to replace the electrons lost in the secondary electron emission. Since insulators do not have electrical conductivity to support the net outflow of secondary electrons from the surface, semiconductors make the best candidate for negative electron affinity operations. [15]

An ideal semiconducting diamond is one that combines doping and monolayer metal surface coatings to display electron negative affinity on the surface. Since diamond has a wide band gap of 5.47 eV, with surface treatments and fabrication, diamond can adapt semi conductivity as a result of impurities incorporated into the bulk through doping.

1.3.1 Semiconductor properties

Semiconductivity can be grouped into two different types:

- 1) P-type behaviour: Boron doped diamond is a common example of materials that displays p-type semi conductivity.
- 2) N-type behaviour: This type of behaviour is originated from the creation of defects. When impurities such as nitrogen, phosphorus, sodium and lithium are introduced to diamond, n-type behaviour will appear. [9]

P-type surface has its E_F nearer to valence band minimum while the E_F of n-type surface chose to be closer to conduction band minimum as demonstrated on figure 1.2.1.2. [9]

1.4 Secondary Electron Emission

Materials that display electron emission from a surface have so many important uses as they can be utilized into electronic devices. The three types of electron emission that can be displayed from a solid surface are thermionic emission, field emission and secondary electron emission. Thermionic emission is the ejection of electrons from a heated material. This mechanism can be used in the application of generating electricity from heat. Electrons emitted from a material under the influence of a large electric field via quantum-mechanical tunnelling are a characteristic of the second type of emission called field emission.

Another type of emission that is intensely the subject of current research is secondary electron emission, which is defined as the release of electrons from a surface upon the bombardment of a primary electron. Diamond surfaces can be adapted to emit more than one electron from the surface in response to irradiation of one incoming electron. Diamond's ability to have a high secondary electron emission yield makes it a demand in areas that are interested at emitting electrons off of a surface. The nature of the secondary electrons arise from the inelastic scattering of the incident electron beam because when an electron beam hits a surface, it will experience energy loss in terms of characters, ionization and secondary electrons. [20]

Electron emission is a three-step process derived by Spicer's in which the first step involves exciting electrons from the valence band by absorption of energy. It is then followed by the transport of electrons through the bulk of the crystal to the surface and lastly electrons will escape from the surface into the vacuum. [9] For secondary electron emission, the primary electrons will penetrate into the surface which leads to the transmission of the internal secondary electrons within the bulk and then finally the escape of the secondary electron emission over the vacuum barrier, as illustrated on figure 1.4. The impacting electrons on a surface will usually lose a certain amount of energy in the bulk, ideally higher than the band gap so that the energy transferred will be able to promote secondary electrons from the valence band to occupy the conduction band. Having the vacuum level E_{vac} lying below the conduction band minimum, which is a characteristic of NEA, will easily emit thermalized electrons into the vacuum as secondary electrons.

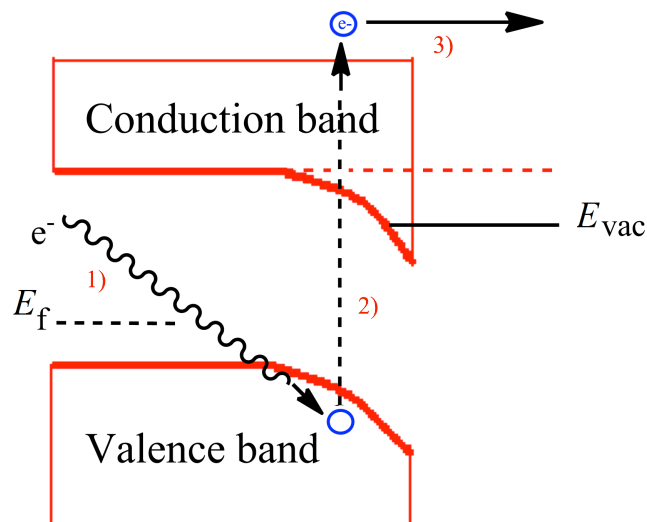


Figure 1.4: The mechanism of secondary electron emission. 1) Primary electron transfers its energy to generate internal secondary electron 2) Transmission of internal secondary electron through the bulk 3) Secondary electron escaping out of the surface. Diagram inspired from [10].

By collecting information from Miller's study, the number of secondary electrons produced was thought to be highly dependent on the energy of the primary electrons. [21] However, the correlation is not as simple as the penetration depth of an incoming electron and the escape depth of the secondary electron generated need to be taken into account as well.

Secondary electron emission has been elaborated differently by different studies. Bandis and Pate [17] have identified the electrons emitted from a NEA surface of diamond is due to the break up of exciton. Excitons are electrostatic combination of electron-hole pairs by Coulombic force. When an electron beam is irradiated to a semiconductor, the incident electron lose energy by creating electron-hole pairs via exciting an electron from the maximum valence band to the conduction band, making a positively charged hole in the valence band. The positively charged hole creates a Coulombic attraction with the electron in the conduction band resulting in a polar nature of excitons. The excited electron then has two possible routes, to either recombine with the hole in the valence band as exciton decay or to be emitted from the conduction band as exciton dissociation. Since excitons are polar in character, they are attracted to the dipole present on the surface-vacuum interface where the break-up of the strong exciton-lattice coupling occurs releasing electrons on the surface into the vacuum as secondary electrons. [17] [8] As the generated internal secondary electrons drift its way through the bulk to the surface, collisions with other bulk electrons result in the formation of more electron-hole pairs until they pile up in the conduction band thus increasing the number of secondary electron yield. [17] [22]

Diamond would be a good candidate as a current amplifier because the secondary electrons are able to move through the bulk efficiently and the presence of a wide band gap enables non-recombined electrons to be emitted from the surface. [4][23]

1.4.1 Secondary electron emission (SEE) yield

Secondary electron emission (SEE) yield, δ is defined ^[4] as the ratio of the total emitted-electron intensity to the primary electron intensity.

1.5 CVD Diamond films

Diamond's high thermal conductivity at room temperature of $2 \times 10^3 \text{ Wm}^{-1}\text{K}^{-1}$ [24] enables it to dissipate heat produced from either the bombardment of primary electron onto the surface or the transport of secondary electrons in the bulk. Transfer of heat needs to be executed efficiently to avoid overheating of a device, which makes diamond beneficial. Diamond based devices would also have a long lifetime as diamond has a mechanical hardness of 90 GPa [24]. Its inertness to chemical and radiation damage allows it to be operated in devices that act as sensors for radiation, specifically β radiation.

The first approach in exploiting the properties of diamond is to make it industrially available so studies can be made on them. Diamond film produced by CVD method was one of the popular approaches to make diamond available for investigations as it can be produced at a low cost to generate different types of crystal based on the current interest. The different types of CVD diamond are ultrananocrystalline (UNCD), nanocrystalline (NCD), polycrystalline (PCD) and single crystal diamond (CSD). The variation in microstructure types may alter the properties of diamond differently in such a way that the thermal conductivity of a PCD can generally be reduced by 25% compared to a SCD due to the presence of more defects in PCD. [25] However, these defects in PCD can be useful in other aspect as it can accommodate higher concentration of contaminants or dopants that may improve the NEA on the surface and increase the probability of electron emission.

Apart from being known as a chemically stable surface, CVD also has a secondary electron emitting surface that can be modified to a certain roughness and orientations to aid in the scattering of incident particles. The high chemical stability of CVD film was displayed when CVD film was used as an anode electrode in KCl electrolyte even over a certain range of voltage. [6]

CVD diamond films are not only easily fabricated at a low cost, but they can also be modified by inserting high levels of doping to improve its conductivity and terminating the dangling bonds on the surface to enhance its emission. [26] The flexibility of a CVD diamond surface has opened a large branch of applications in electronics, as they would be ideally used as electron emitting devices such as magnetrons, electron multipliers, displays and sensors. Incorporating CVD films in the aforementioned devices would only need a low cost as diamond can grow over large areas and only a thin film of a few microns is needed for a high efficiency, hence making it more popular in electronics. The search for an ideal surface that possesses a large NEA surface combined with a high stable SEE yield that can be incorporated to any device of interest is the current motivation in research studies.

1.5.1 Introduction of chemical dopants

Introducing impurities called chemical dopants into the bulk of diamond is able to induce an effective NEA effect on a diamond surface. Changing the chemical composition of the gas phase in the CVD process is one way of adding dopants easily into a diamond lattice during its growth. Dopants like boron and nitrogen are commonly inserted into the bulk of natural diamond to alter it from being an

insulator to a semi conductor. Injecting boron source such as diborane into the gas source during CVD growth process results in the production of a p-type semiconductor of b-doped diamonds. [21]

P-type doping has its acceptor level above the valence band, which accepts electrons from the surface state resulting in the increasing energy of conduction band and bending of minimum band downwards. In an effective NEA caused by doping, it is the bulk conduction minimum that lies above E_{vac} and not the surface conduction minimum. [21] As more band bending occur due to the transfer of electric charges from the surface states to the acceptor levels of boron, the conduction band of the diamond will increase (*cf.* to PEA on diagram 1.2.5.1 and 1.2.5.2) until it leads to a positional change of the vacuum energy level E_{vac} lying below the minimum conduction band E_c to form NEA. [18]

For n-type dopant like nitrogen, the donor levels is located below the conduction band, which indicates that less energy is required to excite electrons to the conduction band minimum, making n-type semiconductors promising materials for electron emission applications. However, nitrogen is electronically inactive due to its donor level located deep beneath the conduction band minimum in the diamond. N-doped diamond samples serve as electrical insulators when the concentration of N is at $\sim 10^{19}$ - 10^{20} cm^{-3} [27] while B-doped diamond samples are conductive. Nitrogen can be introduced to the reactant in its gaseous form of N_2 or NH_3 for it to be incorporated into the diamond structure. [7]

Boron doping provides diamond a certain extent of semiconductivity to reduce the charging effects during photoemission experiments when electrons are lost to the vacuum. [10] [21] There is a specific concentration of boron that can be doped into a sample because Shih reported the decrease in secondary electron emission due to high concentration of dopants when a study made on B-doped CVD diamond was carried out. [15] This might have caused primary electrons to lose some energy via electron-impurity scattering with boron, hence having less energy to emit secondary electrons making electron-impurity scattering the main mechanism for energy loss. The collisions between internal secondary electrons and the dopants were also found to reduce the escape depth of the secondary electrons, which disabled them to escape into the vacuum, contributing to the low yield. Another study [4] also showed there was a large variation on the values of secondary electron emission yield due to different concentration of dopants showing how dependent secondary electron emission is to doping.

1.5.2 Surface treatments

Surface treatments and doping of materials have the ability to reduce the work function of semiconductors, enabling them to possess a negative electron affinity condition. Materials that can achieve the aforementioned conditions would make a good candidate for the use of electron emission in real life applications.

1.5.3 Termination

Changes on the surface of a material can have a large effect on its electronic properties. Bare unterminated diamond surface that has a positive electron affinity can be transformed if the dangling bonds of a diamond surface are terminated with atoms other than carbon as in diagram 1.5.3. The surface will develop a layer of dipole that may induce a NEA effect to improve the secondary electron emission yield.

Termination only occurs on the dangling bond of carbon on the surface of the diamond because in the bulk all the carbon atoms are sp^3 bonded. If the dangling bond is not terminated, cross linkage will be formed leading to a graphite structure, which is a poor secondary electron emitter.^[4] It is worth acknowledging that the electronic properties in the bulk and on the surface are not similar due to different electron densities in both regions. Termination not only can display negative electron affinity, but it also provides stabilization on the diamond lattice.^[4]

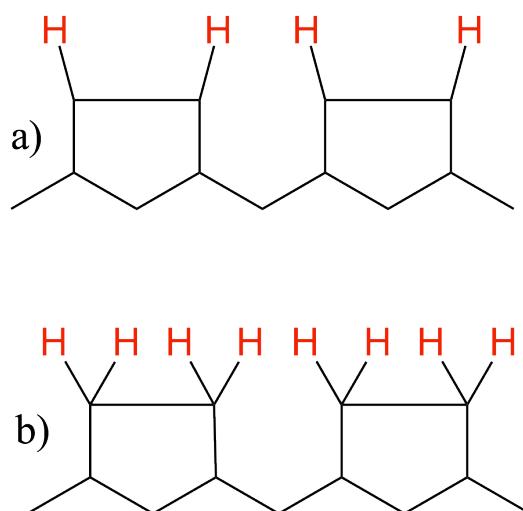


Figure 1.5.3: The dangling bonds on the surface of a diamond terminated by hydrogen. a) Structure of H-terminated C(100)-(2x1) surface and b) Structure of H-terminated C(100)-(1x1):2H surface. Image inspired from ^[13].

Surface chemical modifications

A dipole layer on the surface is established by terminating the surface of a diamond with a more electropositive terminal atom than carbon. As a result, charge redistribution occurs to create a positively charged adatom layer and a small negative charge on the carbon zone. The resulting negatively charged in the carbon lattice can reduce the barrier for electron emission from the surface resulting in a negative electron affinity surface. In reverse, electronegative termination will draw electron density from the conduction band towards the electronegative terminating species, making the electrons less readily available for emission. Surface dipole can have a large effect in changing the work function and the electron affinity of the material therefore different atoms are being used

to terminate the diamond surface so that a surface that can produce the highest electron emission yield can be developed.

1.5.4 Hydrogen terminated

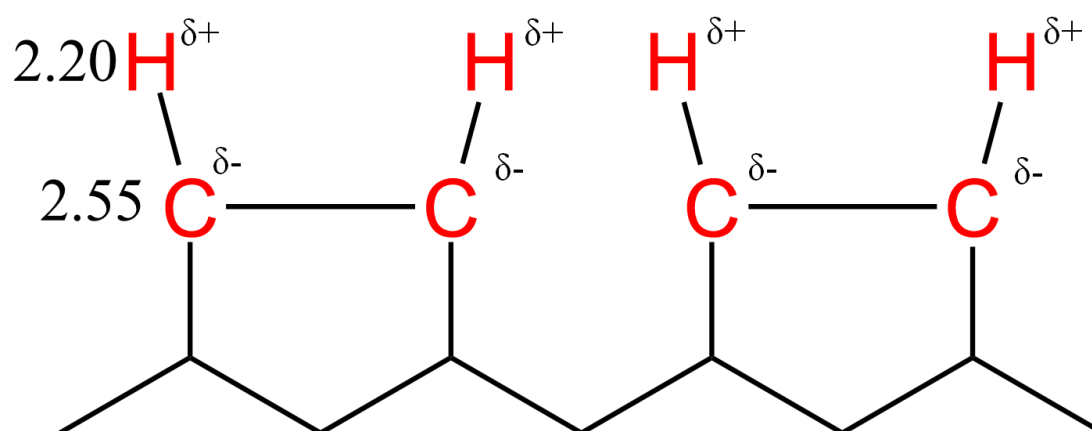


Figure 1.5.4: The difference in Pauling electronegativity between carbon and hydrogen. The hydrogen ad-atom surface has a positive charge relative to the carbon lattice therefore the electrons from the bulk will be attracted to the surface thus releasing more electrons to be emitted into the vacuum.

Reconstruction of the surface of a CVD diamond with hydrogen was correlated to a high yield emission of 12-48, in contrast to the dehydrogenated surface that gave a low yield. [28] NEA effect on the hydrogen terminated diamond was supported previously with recorded NEA values ranging from -2.0 eV to -1.3 eV on a C(100) diamond surface. [29][30][31] The presence of NEA effect on a diamond surface upon terminating with both atomic and molecular hydrogen as carried by Mearini's group [18] was explained by the dipole formed along the polarised bond of C-H caused by the difference in Pauling electronegativity of 2.20 on hydrogen and a 2.55 for carbon as in figure 1.5.4. The positive charge developed on H-termination layer will influence E_{vac} to drop below the conduction band so as to enable the spontaneous ejection of electrons from the surface to the vacuum.

H-terminated surfaces showed negative electron affinity in both N-doped and B-doped surfaces, whilst H-free surfaces displayed positive electron affinity. [9] However only the NEA peak of B-doped (100) surface was significant due to the downward band bending whilst the upward band bending in N-doped (100) surface caused an absence in NEA peak. [15]

Thermionic applications usually require a surface with a work function of approximately 1eV, which makes hydrogen termination undesirable as a device as it has a work function between 2.85-3.90 eV due to the small dipole of the polar C-H bond. [16] [32] Hydrogen terminated CVD is also impractical in devices because its termination gets destroyed at elevated temperatures. Hydrogen desorption would result in a higher work function and low NEA due to E_{vac} being raised above the $\min E_c$. [4] Rapid desorption of the H-terminated diamond is what prevents it from being widely applied in actual devices as it can only portray high yield of emission at low temperature. In contrast, devices tend to function

efficiently only at higher temperatures for industrial purposes. Therefore the search for a surface with a higher NEA nature was needed to overcome the problem with hydrogen coverage degradation.

1.5.5 Oxygen terminated

When the adsorbate atom on the surface is replaced with oxygen termination, electron affinity of the diamond material will increase resulting in a decrease in secondary electron emission. The reduction in NEA on the O-terminated surface is attributed to the Pauling electronegativity of 3.44 on the O atom inducing a larger dipole, however in the reverse direction to the H-terminated diamond. The oxygen-terminated layer is now negative with respect to the positive carbon lattice, which is the opposite to the dipole layer needed for NEA surface. However, O-terminated diamond can enhance the emission properties of the diamond surface by acting as an adhesive layer to other terminal atoms.

1.5.6 Thin films of metal

Fabrication of a monolayer of thin metals like Cu, Ta and Ni on the diamond surface can activate the negative electron affinity of diamond. [21] Although application of the aforementioned metals on diamond can exhibit a stable secondary electron yield and improve the negative electron affinity properties of diamond, formation of carbide with metals can destroy the surface of the diamond and effectively demolish its negative electron affinity nature. [21][33]

A bigger dipole on the surface of the diamond needs to be created so that a strongly positive layer would be formed on top, and a largely negative region beneath it to encourage a large number of electrons to be removed out of the surface. This has brought the subject of alkali metal coating forward to suit the demand of secondary electron emission-based devices because it can form a strong polar bond with other elements, giving a large surface dipole on the diamond. Termination of diamond surface with highly electropositive alkali metals such as Na, K and Cs will improve the negative electron affinity and will release more electrons into the vacuum. [32]

Cesiated surface

Cesiation of the dehydrogenated diamond caused in a higher secondary yield compared to non-cesiated bare diamond condition. [21] The high electropositivity of Cs creates a large dipole forming a strong electron donor on the surface. The only drawback of this preparation was the weakness of the Cs-containing surface. At high temperature, the cesium will be desorbed from the diamond surface. [12] Though cesium is stable in air, the temperature at which the atoms start to desorb is too low for thermionic application. [21]

Alkali-halide films coating

Previously it was done by coating diamond surface with a film of alkali halide and then activating it with electron beam. During the impingement of electron beam on the thin film coated surface, the halogen from the alkali halide will be removed to form a halogen-free surface composing of only a monolayer of alkali metal. This method of terminating alkali metal on diamond resulted in the

formation of electron-beam-activated, alkali terminated (EBAAT) surface. [33] When Ba-coated EBAAT diamond surface was compared to Cs-coated EBAAT surface, Cs group 1 metal had a higher SEE yield value of 30 compared to the Ba-terminated surface having a value of 6 at primary electron energy, E_p of 1.5keV. [33] It was then discovered that group 1 metals produced high stable secondary electron emission which led to the study of CVD diamond with alkali-halide coating such as CsI, NaCl and KCl on various substrates with yield varying from 25 to 45 at primary electron energy E_p of 1.5 keV [33]. According to the group, the activated-alkali termination property produced a large dipole on the diamond surface that attributed to the formation of NEA and a high stable SEE yield. [33] [28] Although Cs-terminated diamond can induce a large dipole to improve the NEA, this surface termination prepared under the EBAAT method was unstable at temperature at above 700 °C. [33][12] As Cs started to desorb from the surface, the NEA was lost to form PEA. [12]

1.5.7 Alkali metal on oxygenated surface

Metal terminated on hydrogen terminated or unterminated diamond surface tends form weak bonds than metal on oxygen terminated surface. [32] Oxygen terminations on diamond act as an adhesive layer to provide stabilization by binding alkali metals strongly on the surface of diamond.

Lithium film on oxygenated diamond surface

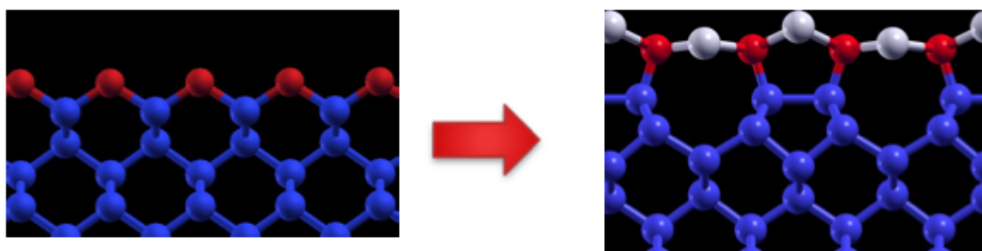


Figure 1.5.7.1: The computed structure of lithium deposited on the O-terminated diamond (Blue atom: Carbon, Red atom: Oxygen, White atom: Lithium). Image taken from [36].

Li adsorbed onto O-terminated surface has a higher binding energy than Li adsorbed to the bare surface of diamond. [35] Among the alkali metals, lithium has the highest binding energy with diamond surface due to its small size, forming a strong bond on the surface as well as stabilizing the surface of diamond. Coating a thin film of lithium on an oxygenated diamond was found to produce a strong negative electron affinity surface due to the ionic character of the Li-O bond. Figure 1.5.7.2 shows the presence of a positive layer of Li and a negative layer on O forming a strong dipole layer on the diamond surface. Although the low ionization energy of Cs in theory would form the strongest ionic bond, however the small size of Li was predicted to give a good coverage due to good overlap with the orbitals on carbon therefore Li termination should result in a better emission. [10] Lithiated diamond has an advantage over previous diamond materials because most of the bonds are weak and can be easily broken by heat.

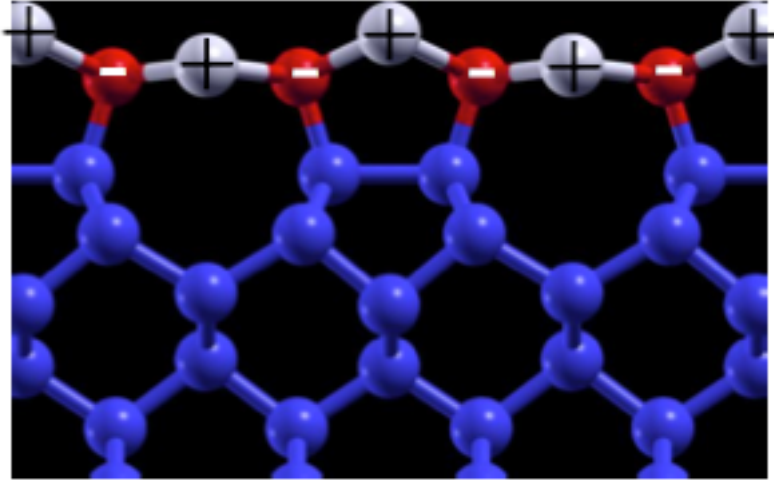


Figure 1.5.7.2: Dipole layer formed on the surface with a positive charge on the Li surface and negative charge on the O layer. Image is modified from ^[34].

1.6 Different types of primary beams

If a suitable diamond surface can be discovered to give a stable high secondary electron emission yield, it can be used for efficient energy production. The diamond-based device would be able to convert high-energy radiation into electrical power, harnessing energy from the radioactive waste generated from nuclear reaction sites. It is a given that diamond has a high resistance towards radiation damage so that it can be utilized as a stable and long-life converter to multiply high energy electron; β radiation to low energy secondary electrons yet at a high current. ^[36]

Radioactive waste radiations that are exploited from radioisotope sources can either be largely penetrating or not, depending on its interaction depth. Beta particles, gamma and high energy x-rays are categorized to have a large penetration depth whilst alpha particles, low energy X-rays and electron beams are recognized to have a small penetration depth. ^[36] For our study, we need to generate electrons within a depth equal to their escape path because study carried out by Trucchi ^[36] confirmed that the secondary electron emission was related to the efficiency of electrons being generated within a small depth under the surface. If we use a highly penetrating radiation, the secondary electrons will require a large escape depth therefore they will just recombine inside the diamond bulk instead of being emitted to vacuum.

Instead of using electron beam to induce secondary electrons, Wieser and his colleagues used H^+ , D^+ , H_2^+ , C^+ , O^+ and O_2^+ slow impact ions previously to bombard the diamond sample and recorded yield between 0.1 and 2. ^[5], which is actually ideal for secondary electron yield in electron emitting devices.

1.7 Aims and objectives:

The aim of this project was to study the influence of the different surface treatments on the secondary electron emission of diamond samples since SEE is known to be highly dependent on surface termination.

In addition, the secondary electron emission yield, δ of H-termination, O-termination, Li-O-termination and LiF-O-termination of diamond were measured.

From section 1.5.3, the formation of dipole was predicted to enhance a negative electron affinity property, which may improve the secondary electron emission of diamond. Therefore the formation of dipole by each surface termination can be deduced based on the SEE yield measurement results.

The next objective of the project was to determine which surface termination gives the highest emission yield so that it can be implemented for electron multiplying applications. Even though some diamond surfaces have been discovered to be able to produce high secondary yield, but they tend to be unstable under continuous electron beam exposure.

First part of the experimental section involved preparing the samples by treating diamond for different surface modifications, followed by the characterization of the samples and finally the study of secondary electron emission.

Part 2: Experimental

2.1 Experimental method:

For this experiment, study was made on only one side of the two different surface roughness on the as-received diamond. The smooth side represented the substrate side, where smaller crystals were deposited. The rough side containing large crystals was believed to be where the polycrystalline diamond growth occurred therefore decision has been made to only consider the rough side of the diamond samples, unless stated. All of the samples provided were boron-doped of the same concentration $\sim 1 \times 10^{20} \text{ cm}^{-3}$, so they were expected to have a semiconductivity character and a degree of negative electron affinity (NEA) due to band bending, as mentioned in section 1.2 and 1.3 earlier.

2.1.1 Sample preparation method

Laser cutting

B-doped polycrystalline CVD diamond samples measuring roughly at $10 \times 10 \times 1 \text{ mm}^3$ supplied from Element Six Ltd. were laser cut using the Oxford Laser Systems laser cutter in the Bristol diamond lab. The high power laser in this machine scribed the as-received samples approximately into $5 \times 5 \times 1 \text{ mm}^3$ dimension. After a total of 3 hours with 80 passes at 1 mm s^{-1} , the samples taken out of the chamber were then snapped physically using cover glasses.

Acid cleaning

The cut samples were then treated for acid cleaning with 100ml of H_2SO_4 under reflux. When acid fuming was observed, KNO_3 (6.5g) was carefully added to the round bottom flask and left for 10 minutes. The samples were then washed with distilled water and left to dry.

Oxygen termination

Four acid cleaned samples were placed on the tray of the Jelight Co. Inc. UVO cleaner (Model no: 42A-220) for 30 minutes at room temperature to facilitate the oxygen-termination of the sample.

Hydrogen termination

Two acid cleaned diamond samples were treated for hydrogen-termination under the microwave chemical vapour deposition (MWCVD) reactor. After air was pumped out of the chamber for 5 minutes to establish a high vacuum environment with a base vacuum value of about $1 \times 10^{-3} \text{ Torr}$, the sample was then exposed to hydrogen plasma treatment with hydrogen gas flow rate at 500 sccm, a pressure of 80 Torr at $600 \text{ }^\circ\text{C}$ and microwave power of 1014 W for 20 minutes.

Lithiation

Samples that have been oxidized by acid cleaning method and ozone cleaner were sent to be lithiated using the Balzers 510 coating machine located in the Physics Building, University of Bristol. Atomic lithium was deposited by thermal evaporation of lithium metal on to the surface of the sample. A quartz crystal monitor QSG 201 was attached to the thermal evaporation gun to monitor the thickness of the lithium film deposition in situ. The thickness at which Li diffused onto the diamond samples was set to be at 550 Hz, which was approximately equivalent to 100nm. Excess lithium was then removed by dipping the sample in triply distilled water; Milli-Q water for 5 seconds to achieve a monolayer of lithium on the surface.

Lithium fluoride deposition

The deposition of lithium fluoride (LiF) onto another set of samples; acid cleaned sample and ozone treated sample was carried out using the same set-up on the Balzers 510 coating machine. For this process, solid LiF was used as a source to thermally evaporate LiF to deposit a film of approximately 30Å at 37.5 Hz. The LiF layer was left in excess on the sample.

2.1.2 Sample characterization method

Energy-dispersive X-ray spectroscopy

Elemental analysis of the surface sample by energy-dispersive X-ray (EDX) spectroscopy was carried out under Hitachi S-2300 Scanning Electron Microscope in the Interface Analysis Centre (IAC), University of Bristol and the X-ray detector used was supplied from Link Analytical Ltd.

Contact angle measurement

Contact angle measurement was performed using the KRÚSS Drop Shape Analysis System DSA100E equipment in the KRÚSS Centre in the School of Chemistry, University of Bristol. Deionized water of 1µl was dropped onto the samples in air using a micro syringe controlled by a program. DSA4 software was used to calculate the contact angle through analyzing the shape of the drop profile. After contact angle measurements were taken, samples were baked up to 200 °C to remove any moisture adsorbed on the diamond surface.

Conductivity test

A simple conductivity test was measured out by a digital voltmeter; Caltek Instrument CM1502. The probes were placed at the two points on the sample according to the diagram on figure 2.1.2.

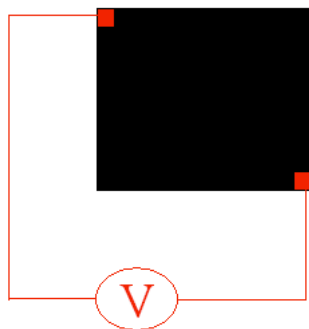


Figure 2.1.2: The two red points showed the positions of the probe where the resistance measurement was taken.

2.1.3 Secondary electron emission studies

Scanning electron microscope

Scanning electron microscope; Hitachi S-2300 was used as a qualitative comparison of emission from different surface terminations based on the surface brightness.

Secondary electron emission yield measurement

Faraday Cup was set-up in the scanning electron microscope JEOL Scanning Electron Microscope JSM-6100 in the Interface Analysis Centre, University of Bristol as seen on figure 2.1.3.1, enabling the secondary electron emission yield measurement to be taken. The electron gun from the SEM was controlled to produce incident beam current ranged from 4×10^{-12} to 1×10^{-11} A and primary electron beam energy, E_p from 0.6 to 10 keV. E_p below 0.6 keV produced incident current value comparable to the noise current of the system; therefore the lowest energy beam current used to evaluate the yield was capped at this value. A high vacuum condition was set up to ensure a minimum amount of background noise collection.

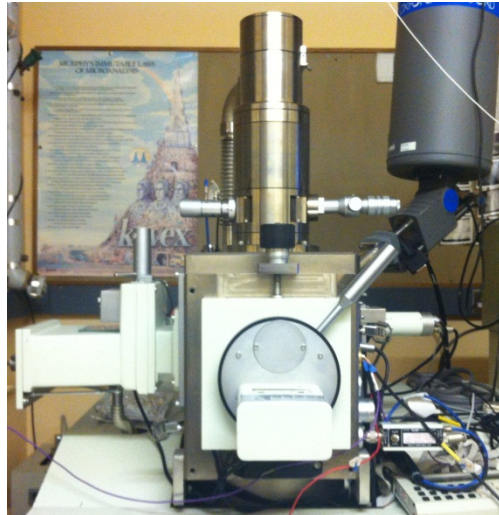


Figure 2.1.3.1: JEOL JSM-6100 SEM used to place the Faraday cup for SEE yield measurement. This set-up was located in the Interface Analysis Centre Lab, University of Bristol.

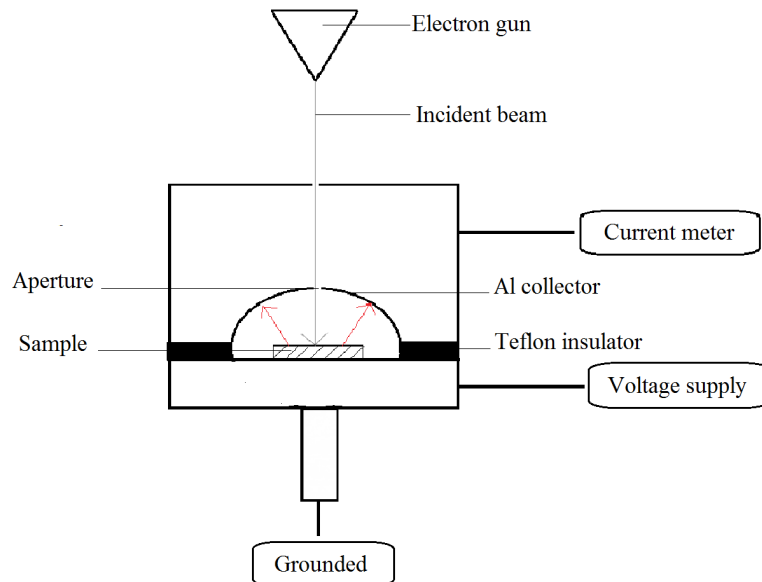


Figure 2.1.3.2: The schematic diagram of the assembly of Faraday cup found inside the chamber of the set-up. The principal measurement of the set-up above involved recording the current generated from a sample under variable primary beam energy, E_p .

2.2 Introduction

2.2.1 Sample preparation

2.2.2 Cleaned samples

The acid cleaning was believed to not only remove the impurities on the surface but also to chemically oxidize the diamond surfaces to form O-terminated sample. The graphitic features that might have been formed during the laser cutting process would also be removed after the acid cleaning.

2.2.3 Ozone cleaner

The Jelight Ozone Cleaner has a high intensity low-pressure mercury vapour UV grid lamp installed in the system. UV radiation at a wavelength of 254nm irradiating the sample would dissociate any contaminant molecules on the surface with occasional generation of O₃ ozone gas in the atmosphere inside the set-up. UV radiation in the cleaner has the right energy to dissociate the ozone gas enabling the reactive oxygen atoms to abstract the surface of the diamond. Hence, not only this technique cleaned the surface by removing contaminants when they absorbed UV light, but it also resulted in O-terminated diamond surface.

During the oxidizing process of a diamond surface under the ozone cleaner, oxygen atom may abstract the CH₂ bonds on the (100) facets and CH bonds on the (111) facets of H-terminated diamond sample. [37] Oxygen would have a choice to adsorb to the (100) surface in either the carbonyl or ether manner. The carbonyl structure is when the carbon on the surface site forms double bond with oxygen and the ether manner is when a single bond is formed between carbon and oxygen where oxygen acts as a bridging site between two adjacent carbon atoms on the surface. [32] As for the (111) facet, oxygen would be inserted into the C-H bond forming C-OH bond. Since the percentage of facets for the samples were not determined, the predicted coordination for the O-terminated surface is shown in figure 2.2.3.



Figure 2.2.3: Cartoon diagram of how O-terminated sample would look like under incomplete oxygenation treatment, with the presence of H-termination.

2.2.4 H-Termination

The process of rehydrogenating the dangling terminal bonds of diamond surface is termed as hydrogen termination. In the MWCVD reactor, heating the sample up to 600°C should break all the bonds on the diamond surface, be it with hydrogen or other elements, to achieve a bare diamond surface. After exposing

the bare diamond surface, the environment was filled with hydrogen gas heated and excited by microwave to form hydrogen plasma. The activated hydrogen plasma was believed to reconstruct the bonding on the diamond surface leaving a top layer of hydrogen atom. [38]

2.2.5 Lithiation

Lithiation was only carried out on the O-terminated sample because Li would form a stronger bond with oxygen than it would form with hydrogen. Lithiation has also been proven to induce NEA effect and hence reduce the work function of a diamond surface. [32] Although Li would form the smallest dipole with O compared to the other group 1 metals, its small size gives it an advantage to form a stronger bond.

2.2.6 Li-F deposition

LiF was also found to be able to lower the work function of a diamond surface. Previously [39], H-terminated and O-terminated diamond with positive electron affinity surfaces were transformed to negative electron affinity surfaces upon the deposition of LiF on the surface, reflecting the effect of a strong dipole on the surface due to a strong dipole moment of 6.326 ± 0.633 D [40] on LiF. In this experiment, LiF was deposited onto O-terminated sample, for the same reason Li-O-terminated sample was formed. The strongly polarized Li-F bond was predicted to create a dipole either directly with the carbon on the diamond surface, that is if fluorine was able to replace oxygen or through the oxygen center that acts as an adhesive on the O-terminated diamond surface. With this said, the exact coordination of LiF to the O-terminated surface has not been discovered yet. But for now, lithium fluoride on oxygen-terminated diamond can be treated as LiF film deposited on O-terminated as shown on the diagram of figure.

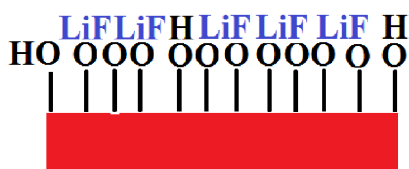


Figure 2.2.6: Cartoon diagram of LiF deposited on O-terminated diamond surface.

2.2.7 Sample characterization

2.2.8 Energy dispersive X-ray spectroscopy

Energy dispersive X-ray spectroscopy (EDX) makes use of X-ray as an analytical tool to characterize the elemental composition of a sample. The incident electron beam from SEM will excite a ground state electron in the lattice, creating a hole that will induce electron from a higher energy shell to replace this hole. The energy given out during the movement of electron from a higher energy shell to fill in the hole is given out as an X-ray, which will then be converted into a voltage signal. Due to the unique atomic structure of different atoms, they will

generate different energies of X-ray based on the energy gap between shells. Therefore EDX can determine the origin atom of the X-ray allowing the identification of atoms found on the surface.

2.2.9 Contact angle measurement

To study the wetting and the polar characteristics of a surface, the contact angle of a water droplet on a sample was taken. The angle θ is defined between the contact line of the water droplet on the solid surface and the tangent to the liquid-air interface on the droplet as in figure 2.3.3. Since contact angle of a sample usually rely on the polarity of the sample surface, θ values of 0° to 90° corresponded to a hydrophilic surface due the water droplet being attracted to the surface while hydrophobic surface would have θ values from 90° to 180° because the water droplet would not be interacting with the non-polar surface.

2.2.10 Conductivity test

The conductivity test was carried out using a 2-point probe as a preliminary test of its surface resistance.

2.2.11 Secondary electron emission studies

2.2.12 Scanning Electron Microscopy

In this study, the operation of SEM was applied to study the secondary electron emission properties. When incident electrons hit the sample, weakly bound electrons near the surface that have low energy will be emitted as a signal to draw an image of a sample. ^[10]

SEM equipment needed to be under high vacuum conditions because the contamination of gases can damage the surface of a sample by desorbing the weakly terminating atoms on the diamond surface.

The first test to quickly asses the property of emission from a surface was by comparing the different surface brightness under the SEM. SEM was used because it can act as a source to produce low energy electrons of 0.01 keV to 10 keV so that the energy lost from the primary electrons upon collisions can be transferred to electrons in the solid near the surface to be emitted as secondary electrons. Based on the intensity of the brightness of each sample, a brighter sample indicated more secondary electrons emitted.

2.2.13 Secondary electron emission yield measurement

Upon the bombardment of primary beam onto the sample in the Faraday cup as shown on figure 2.1.3.2, electrons were emitted from the sample in all directions and collected by a detector lining the internal side of the hemispherical cup of the Faraday. The electrons collected will be measured in terms of emission current read off by a current meter.

Bias voltage was applied between the sample and the detector to overcome a common complication in this set up, where slow moving electrons emitted out were deposited on the surface. Instead of being collected by the detector, these electrons formed a cloud of electric charge region in the interelectrode space

between the surface and the detector, which is called the space charge effect. Space charge may be observed since rough side of the diamond was utilized in this experiment, where the charge might have built up on the rough edges if bias was not implemented. The charge build up may impede other electrons from being emitted from the surface, acting as a barrier to emission. ^[28] Usually bias voltage would be used to overcome the work function difference between the sample and the collector but in this situation ^{[41][22]}, probing a positive bias of +20 V on the sample will force the emitted secondary electrons to return to the diamond surface while a negative bias of -20 V will repel the secondary electrons away onto the detector for the evaluation of secondary electron emission (SEE) yield, δ , using equation 2.2.13.

The secondary electron emission yield, δ , is defined as the ratio of current of all emitted electrons leaving the surface of a sample to the ratio of current of incident electrons. δ is typically plotted as a function of the primary energy E_p .

$$\delta = \frac{I^- - I^+}{I}$$

Equation 2.2.13: The equation that defines the secondary electron emission (SEE) yield, δ . Where δ is the secondary electron yield, I^- is the current when a negative bias voltage is applied, I^+ is the current in the presence of a positive voltage bias and I is the incident current.

2.3 Results and discussion

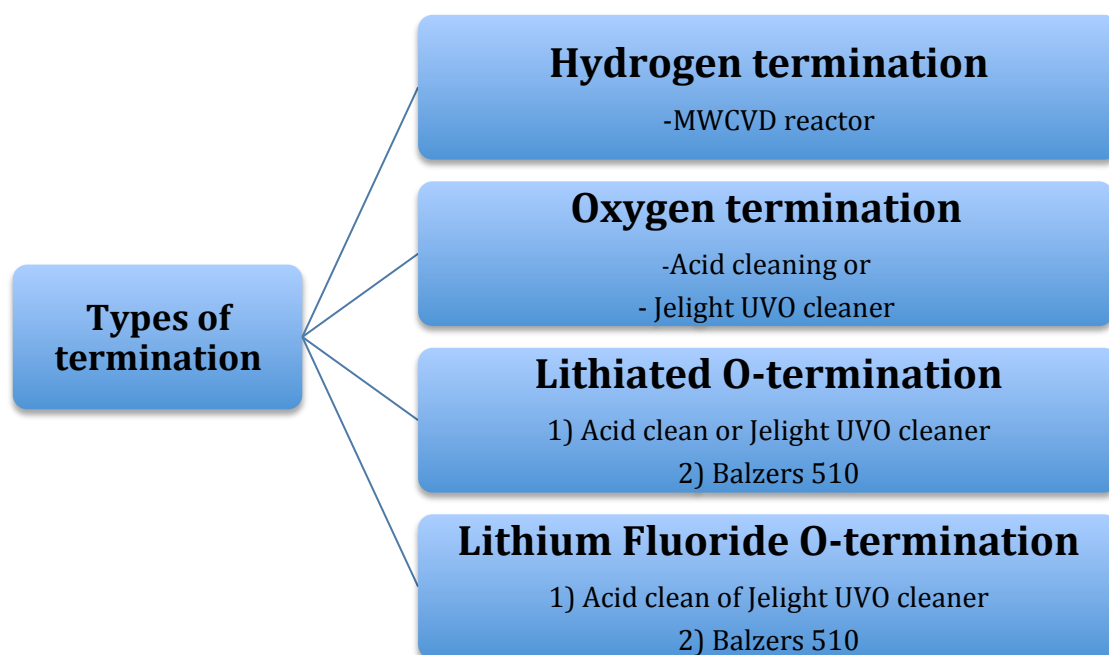


Chart 2.3: The four types of surface terminations prepared for this experiment.

The four types of surface terminations prepared in this experimental section were H-terminated, O-terminated, Li-O-terminated and LiF-O-terminated as displayed in chart 2.3. The O-terminated samples were prepped by two different methods; acid cleaning and ozone cleaned. The O-terminated samples were then further treated for Li and LiF deposition. The surface treatments that each sample has undergone are summarized on table 2.3 below for easier reference.

Name of sample	Predicted type of surface termination	Treatments
Test	Mixture of H-term and O-term	Untreated
A5	O-term	Acid cleaned
O5	O-term	Acid cleaned, followed by ozone treatment
H5	H-term	Acid cleaned, followed by H-termination in the MWCVD reactor
O4	O-term	Acid cleaned, followed by ozone treatment
H4	H-term	Acid cleaned, followed by H-termination in the MWCVD reactor
A1	Li-O-term	Acid cleaned, followed by lithiation
O1	Li-O-term	Acid cleaned, ozone treatment and then followed by lithiation
A2	LiF-O-term	Acid cleaned and followed by Li-F deposition
O2	LiF-O-term	Acid cleaned, ozone treatment and then followed by Li-F deposition

Table 2.3: A summary of the different treatments on each sample. The size of all the diamond samples are roughly 5 x 5 x 1mm³.

2.3.1 Sample characterization

The samples were first characterized to confirm the success of the surface treatments.

2.3.2 Energy dispersive X-ray spectroscopy

The EDX curves of all the samples showed a large peak at 0.277 keV representing the signal emitted for C (6) K α shell. This was a result of X-ray emission of an electron from a K shell of carbon that has been ionized. Samples A4, O4, A2, O2, A1 and O1 were all believed to have oxygen present due to the acid cleaning of A4, A2 and A1 and ozone treated O4, O2 and O1 samples that have been treated for oxygen termination. However all the spectra of the aforementioned did not show a significant signal at 0.525 keV which would be a characteristic energy of X-ray generated by O (8) K α (see appendix 2.6.1). It was plausible to assume the detector was incapable of collecting X-rays generated by oxygen atom on the sample because it was too light. The limitation of this EDX analysis was also due to the low resolution of the detector, which accounted for the very low count of only 40-60 counts per second during its operation.

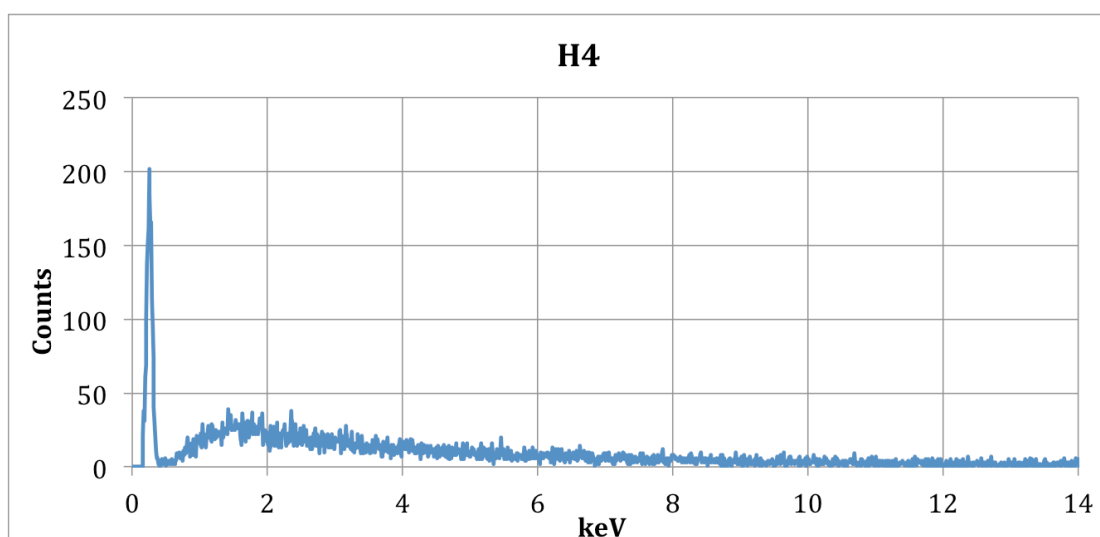


Figure 2.3.2.1: EDX spectrum of H-terminated sample H4.

Judging from the spectrum of H-terminated sample on figure 2.3.2.1 and the set of spectra on appendix 2.6.1, the shape of the curves are similar thus they can be pinned as background noise. With an exception for the LiF-containing samples A2 and O2 spectra on figure 2.3.2.2 and 2.3.2.3, there was a small peak present at 0.677 keV. Although the peak at this particular energy displayed a low intensity, the signal cohered with X-ray energy emitted from F(9) K α shell. The peak at 0.677 keV therefore concluded the presence of Li-F on the O-terminated diamond, which certified the success of LiF lamination via thermal deposition.

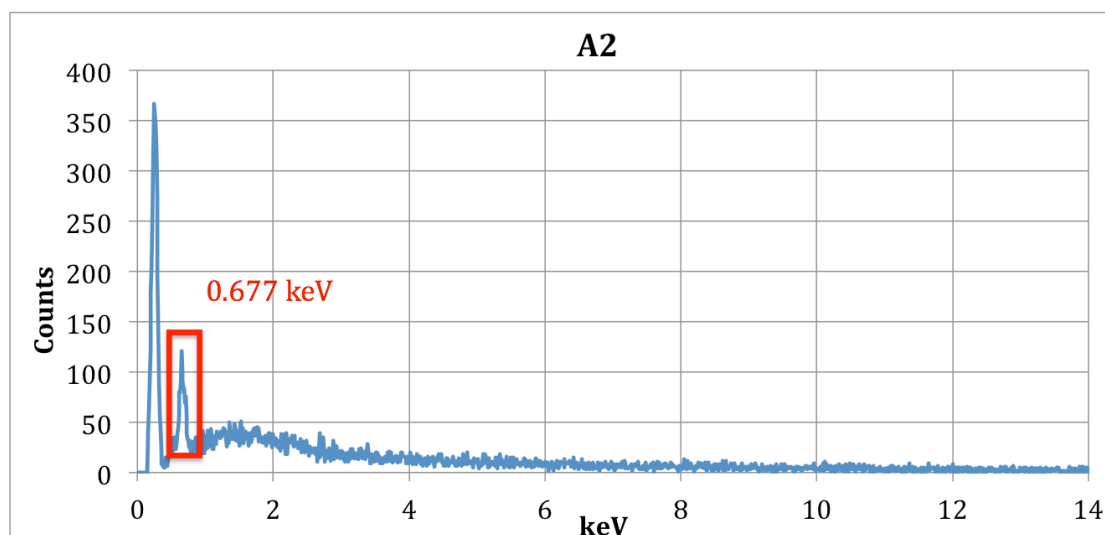


Figure 2.3.2.2: EDX data for LiF-O-termination; A2 sample. O-termination was obtained by acid cleaning.

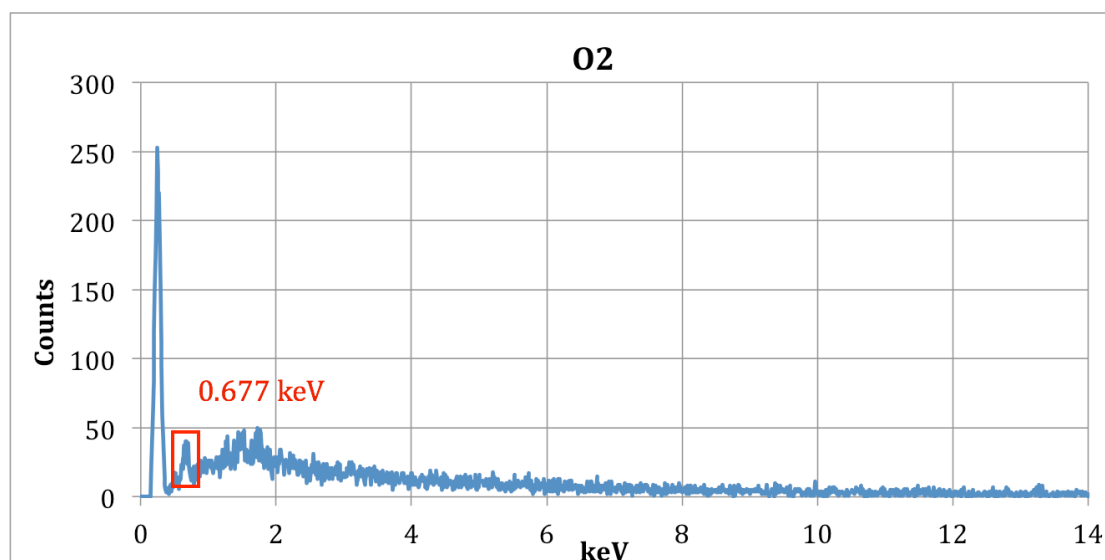


Figure 2.3.2.3: EDX data for LiF-O-termination; O2 sample. O-termination was obtained by ozone cleaning.

EDX spectroscopy is generally unequipped for detecting elements lighter than boron; therefore signal for lithium from the lithiated samples A1 and O1 would not be observed. Instruments with a higher sensitivity like XPS would be required to detect Li and O on the surface.

2.3.3 Contact angle measurement

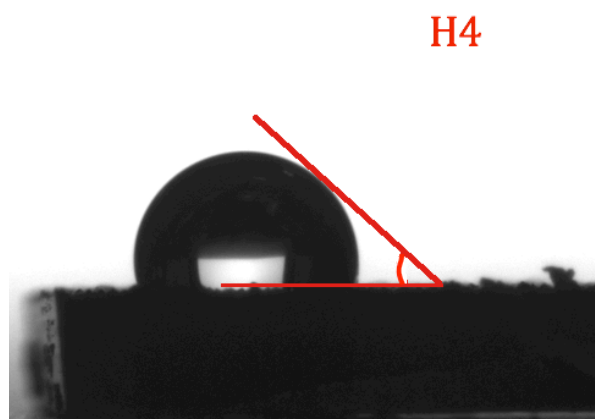


Figure 2.3.3: A drop profile of a H-terminated sample (H4), which defined the contact angle θ .

Name of sample	Contact angle θ (L) / °	Contact angle θ (R) / °
Test	101.5	101.8
A5	75.6	78.5
H4	103.7	102.2
O4	61.3	61.3
A1	88.7	88.5
A2	12.5	12.5

Table 2.3.3: Contact angle values on the different samples. This table shows the contact angle values, θ , on the left (L) and the right (R) side of the drop.

The rough surface of the samples resulted in deviated values of contact angle on the left and right side of the drop as shown in table 2.3.3. The difference in contact angle of a H-terminated diamond (H4) from 103.7°/102.2° to 61.3°/61.3° on the O-terminated diamond (O4) indicated the expected change from hydrophobic surface to hydrophilic terminated surface, which agreed with literature. The literature contact angle value of H-terminated diamond by hydrogen plasma was around 74°-93°, while the O-terminated diamond was found to be at a range of 30° to 60° due to the different method of oxidizing the diamond and can go up to < 5° if a fully oxidized surface is achieved. [38] [42][43] [44] [45] O-terminated surface was hydrophilic due to the presence of hydrogen bonding between water and oxygenated surrounding. Meanwhile, the hydrophobic character of the H-terminated sample can be explained by a smaller extent of hydrogen bonding due to steric hindrance.

Comparing the untreated diamond (Test) with acid cleaned sample (A5) and ozone cleaned (O4), sample O4 has the lowest contact angle of 61.3°/61.3° indicating that O4 might have the most oxygen surface coverage. The slightly higher values of 75.6°/78.5° on sample A5 signified a presence of hydrophobic H-terminations. It was clear that the contact angle of acid cleaned sample demonstrated some oxygen coverage on the sample due to the etching work of HNO₃ from the acid washing treatment upon exposure to atmosphere [38], however the oxygen coverage might have not been as extended as the ozone treated sample O5. While EDX was unable to confirm the presence of oxygen on

all the O-containing samples, the results from contact angle calculation concluded that the samples were successfully transformed to O-terminated sample.

In theory, fluorine on LiF –deposited surface would be expected to introduce a certain amount of hydrophobicity. In contrast to the literature value of F-terminated diamond of 93° , LiF deposited on oxygen terminated sample A2 showed the most wetting behavior for having the lowest contact angle compared to all the samples. Moreover, LiF-O-terminated sample would have the most polar, hence hydrophilic surface. Contact angle of 12.5° may be used as a first pointer to conclude the presence of dipole on the surface of the LiF-O-terminated sample. Li-O-terminated sample (A1), on the other hand, showed a hydrophobic character similar to H-terminated sample, making them possible to be grouped together to have a positive layer on the top surface according to figure 1.5.4 and 1.5.7.2. LiF-O-terminated sample being hydrophilic would mean it has a similar surface character to the O-terminated diamond. This may act as a guide that fluorine has been incorporated on to the O-terminated diamond surface in such a way to form a negative top surface. Though the exact coordination cannot be determined from contact angle measurement alone because contact angle could only tell the polarity of a surface. Surely contact angle would also be dependent on the homogeneity of the functional group coverage and can be influenced by the roughness of the surface. [46]

2.3.4 Conductivity test

Due to the simplicity of the 2-point probe test, the values fluctuated at different positions on the surface, therefore an average of measurements were taken..

Name of samples	Surface termination	Average resistance on the rough side / Ω cm
Test	Mixture of H-term and O-term	48.8
A1	Li-O-term	38.0
A2	LiF-O-term	40.8
A5	O-term	42.2
01	Li-O-term	51.0
02	LiF-O-term	33.9
04	O-term	38.9
05	O-term	74.2
H4	H-term	35.4
H5	H-term	22.2

Table 2.3.4: shows the averaged value of resistance on samples treated differently.

The resistance values on table 2.3.4 only indicated the surface resistance, not the bulk resistance introduced by the boron dopants. Usually an undoped diamond would have a high electrical resistivity with typical values of above $10^8 \Omega\text{cm}$ [37] when measured using a 4-point probe. A pattern could not be drawn due to the inconsistency of the values, even on samples that have undergone similar

treatment. To investigate further on the conductivity of the samples having different treatments, a 4-point probe would be able to record more accurate resistance values. However, the samples having dimensions of $5 \times 5 \times 1\text{mm}^3$ were too small for the 4-point probe set-up. Since the samples were bought in and the specifications were known anyway, confirmation was not needed for a low resistance data, as the samples were already boron-doped from the supplier.

2.3.5 Secondary electron emission studies

2.3.6 Scanning Electron Microscopy

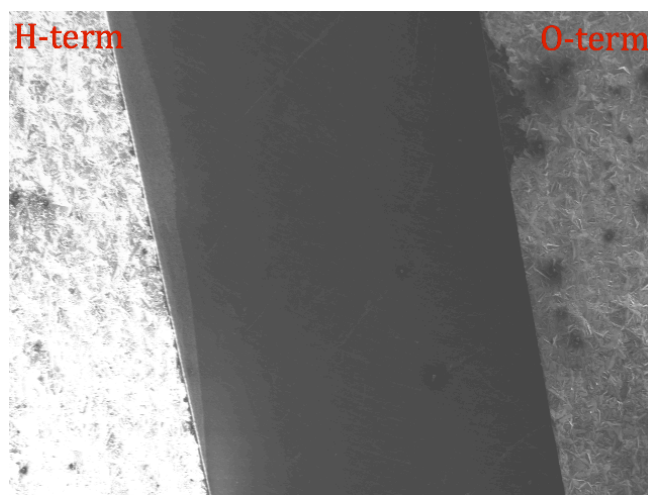


Figure 2.3.6.1: SEM image of H-terminated sample on the left and O-terminated sample on the right showing the difference in brightness.

According to the low magnification SEM image on figure 2.3.6.1, H-terminated sample appeared brighter than the O-terminated. The contrast in brightness of the samples was due to H-terminated sample emitting more electrons than O-terminated sample from its surface assisted by the enhanced NEA property of H-terminated surface as mentioned in section 1.5.4.

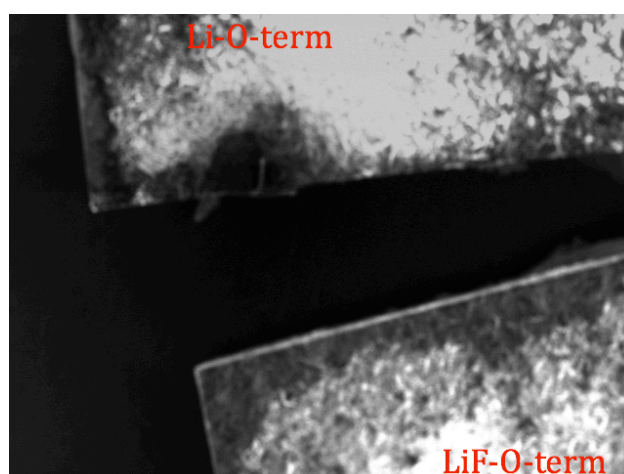


Figure 2.3.6.2: Li-O-terminated sample at the top and LiF-O-terminated sample at the bottom.

Meanwhile, the brightness of Li-O-terminated sample was similar to LiF-O-terminated sample therefore it cannot be concluded which surface was better at ejecting secondary electrons. Similarly, there was no significant difference in brightness between Li-O terminated sample and O-terminated sample on figure 2.3.6.3. Drawing conclusion from these observations, H-termination has a higher intensity of brightness than all three O-termination, Li-O-termination and LiF-O-termination collectively.

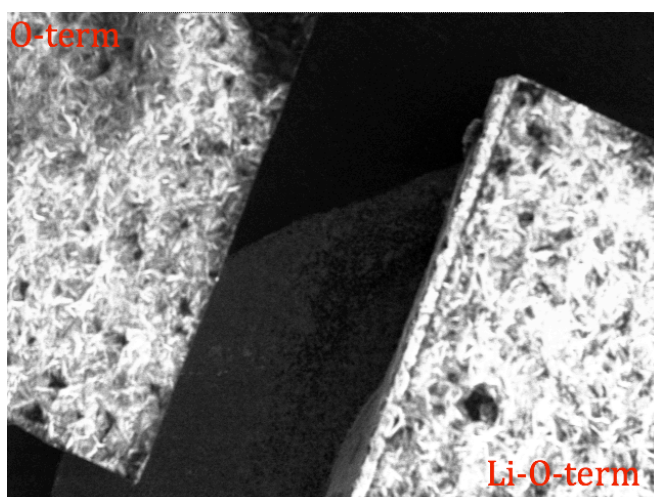


Figure 2.3.6.3: O-terminated sample on the left aligned next to LiO-terminated sample on the right.

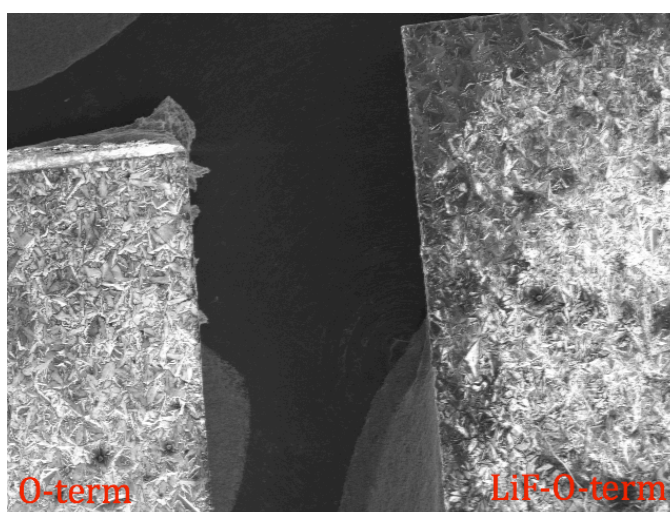


Figure 2.3.6.4: Result showing the similar brightness of O-terminated sample on the left with LiF-O-terminated sample on the right.

On a side note, the dark spots on the H-terminated sample shown on figure 2.3.6.5 displayed a non-uniform intensity on the surface indicating the surface terminations did not give a good coverage throughout the sample. As for O-terminated sample, it was anticipated to appear dark under the SEM, however there was area on the surface appearing brighter than it should on figure 2.3.6.6. This inconsistency of brightness may be due to incomplete oxygen coverage.

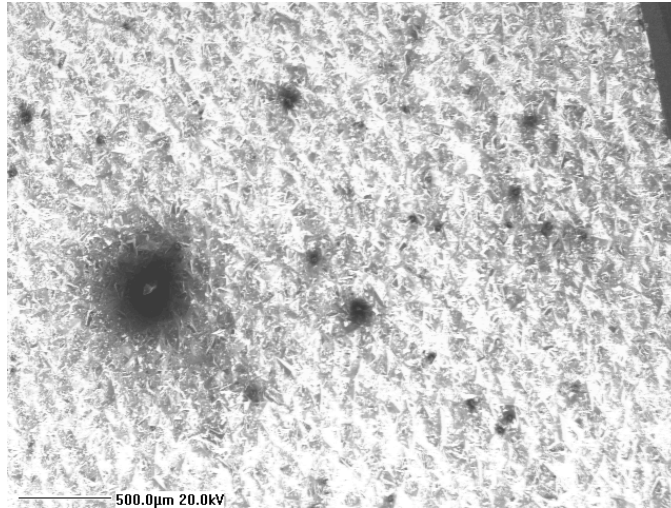


Figure 2.3.6.5: H-terminated sample under the SEM at low magnification showing the non-uniform brightness intensity.

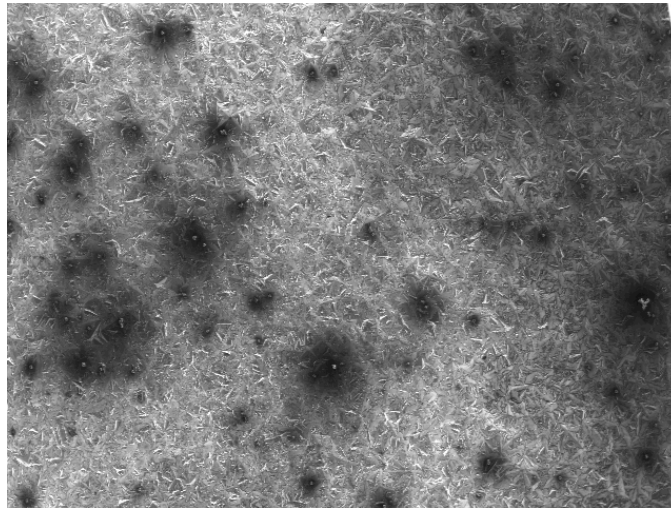


Figure 2.3.6.6: O-terminated sample showing inconsistency of dark spots on the surface.

While the comparison between H-terminated and O-terminated diamond agreed with literature ^[45] and also correlated with the dipole theory as mentioned in section 1.5.3, a clear-cut conclusion cannot be drawn out of the relative brightness between the O-terminated, Li-O-terminated and LiF-O-terminated due to the limited number of samples that can be compared per snapshot. The inconsistent brightness across the surface samples gave an indication that the degree of surface terminations was poor throughout the sample. The result from the SEM was undoubtedly only a qualitative assessment regarding the SEE of the samples therefore measurements of the SEE yield ought to be carried out to get a qualitative dimension.

2.3.7 Secondary electron emission (SEE) yield measurement

For a quantitative assessment on the emission properties, the secondary electron emission yield has to be studied. SEE yield of all the samples in this experiment were measured using the Faraday cup set-up as in figure 2.1.3.2.

The SEE yields of four different surface terminations were plotted as a function of primary beam energy E_p as shown in figure 2.3.7.1. H-terminated sample has the highest SEE yield for the whole range of E_p measured, unexpectedly followed by Li-O-terminated. At 0.6 keV the yield of H-terminated surface was 5.88, compared to the yield of Li-O-terminated sample, which was 3.86. Clearly from this observation it can be concluded that H-terminated was better at emitting secondary electrons compared to Li-O terminated, LiF-O-terminated and O-terminated samples. This result reinforced the observation made in the brightness test in section 2.3.6.

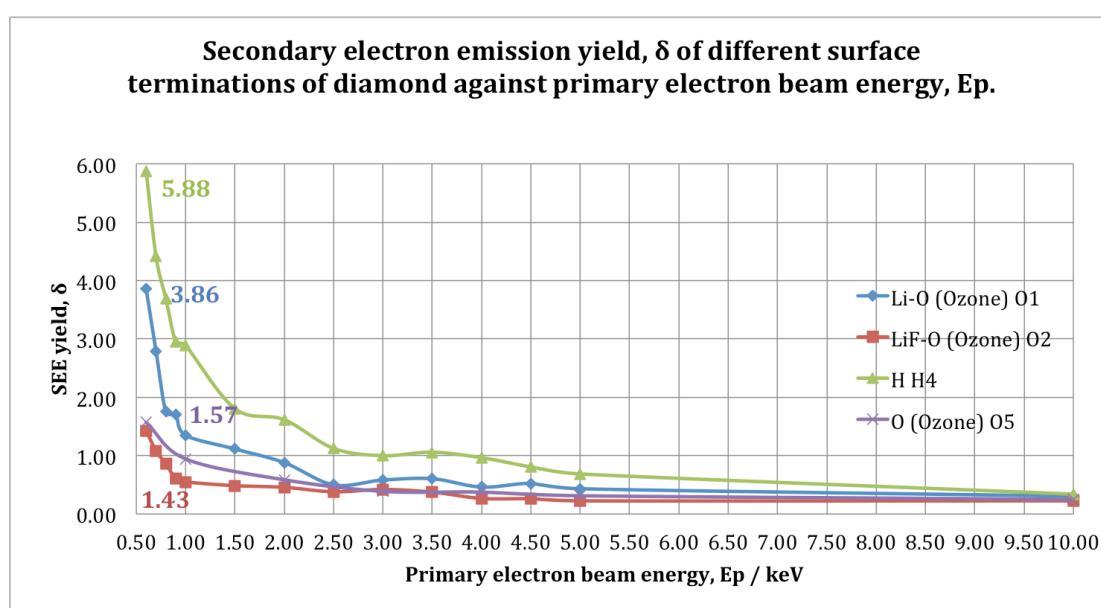


Figure 2.3.7.1: The secondary electron emission yield data of H-terminated sample in green, Li-O-terminated sample in blue, LiF-O-terminated sample in red and O-terminated sample in purple. Yields at $E_p=0.6$ keV are shown for all the four samples.

For O-terminated sample, it was predicted to be the poorest secondary electron emitting surface due to the reverse dipole layer formed on the surface according to section 1.5.5, which may have destroyed the NEA surface. However it was unexpected for Li-O-terminated and LiF-O-terminated samples to have lower emission than H-terminated sample because they were hypothesized to have formed a stronger dipole on the diamond surface, which was predicted to enhance the NEA property of the surface, directly improving the secondary electron emission. However since we were only studying the emission yield of the surface without observing the actual NEA and work function values of each surface, there would be no correlation between the size of the dipole to the degree of NEA on the surface that may have affected the emission yield. At low E_p of below 3 keV, H-terminated started to have yield of bigger than 1, making it a

good surface for electron multiplying devices. The curve of LiF-O-terminated sample and O-terminated sample almost overlapped one another at higher E_p .

Referring to figure 2.3.7.1 again, the yields for LiF-O-terminated and O-terminated samples at $E_p=0.6$ keV are 1.43 and 1.57 respectively. The yields of these two surface terminations were quite close; therefore a comparison has been made between two LiF-O-terminated samples with the O-terminated sample as shown on figure 2.3.7.2. Sample A2 and sample O2 acquired the same LiF-O-terminations, the only difference was how they were oxidized prior to LiF deposition; A2 was acid cleaned while O2 was ozone treated. Above $E_p=3.5$ keV, sample A2 has the highest emission followed by O-terminated sample and finally sample O2 being the lowest. The curves interchanged at the region between $E_p=2$ keV and $E_p=3.5$ keV. At 0.6 keV O-terminated led with a yield of 1.57 while the two LiF-O terminated samples only had yield values of 1.43 and 1.08. This can only be supported with a valid explanation if the coordination of LiF on the surface was known. The lithium should have enhanced the emission of the oxygen terminated diamond sample however it did not, in fact the LiF-O terminated sample was poorer at emitting electrons compared to O-terminated sample indicating there was no evidence of a strong dipole layer formed by the LiF layer and the carbon lattice of the diamond sample. First assumption made regarding the low yield from LiF-O-terminated sample was due to the thick LiF film deposited in excess on the diamond. It may have just been laminated on the surface without forming a bond to the O-termination of the diamond, eliminating the formation of a dipole layer. In addition, excess LiF may have caused its work function to dominate on the diamond surface. Instead of having a work function of diamond on the surface, the work function of LiF might have been observed, similar to a previous study ^[47]. The work function of LiF (~ 2.4 eV) on the surface must have been too high for secondary electrons to overcome the barrier to emission. Second reason to explain for the low yield of LiF-O-termination, the primary electron beam may have bombarded a region of O-terminated that has no LiF deposited on the surface of the sample. However the second assumption would most likely be rejected as repeat of measurements for the same surface termination, but of a separate sample, gave similar yield values regardless.

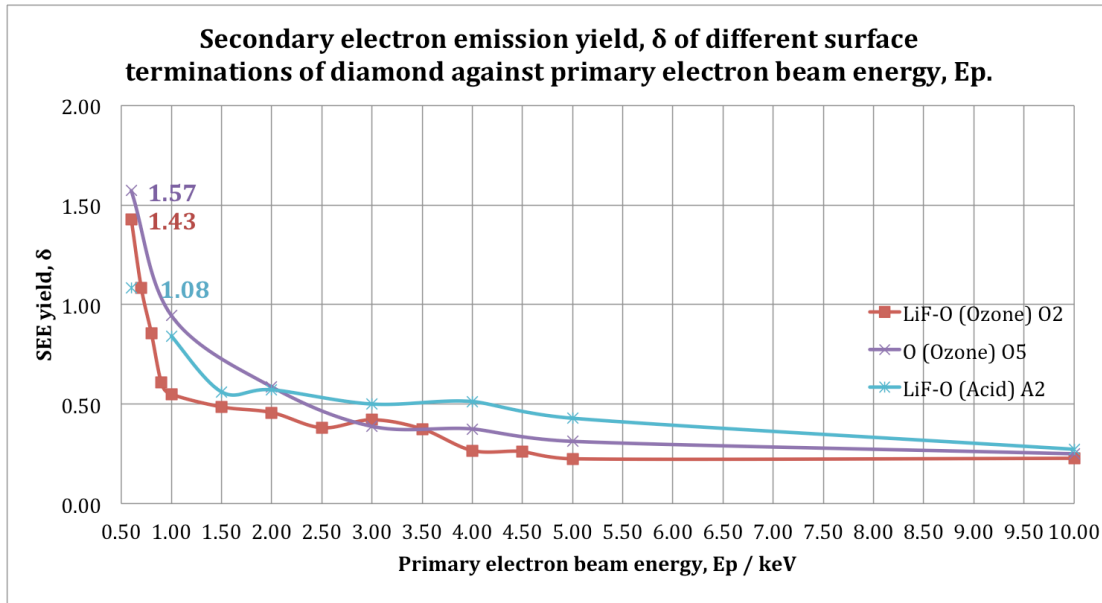


Figure 2.3.7.2: Comparison of the yields of LiF-O-termination with O-termination. There were two samples of the same surface termination (red and purple), only differing by the process of oxidizing the sample prior to LiF deposition. Red curve was oxidized by ozone cleaner while the blue curve was oxidized by acid cleaning.

Graph on figure 2.3.7.3 showed two different samples of Li-O-terminated diamond. The blue curve was of the O1 sample prepared in this experiment while the orange curve represented a B-doped Li-O-terminated diamond obtained externally from a colleague studying in the same area. For argument purposes, the Li-O-terminated diamond was labeled as 'external'. The SEE yield measurement for the external diamond was attained to validate the yield of Li-O-terminated sample O1 since it did not agree with the hypothesis made in section 1.5.7. Li-O-terminated diamond was expected to have a higher yield compared to H-terminated sample due to a stronger dipole layer from the ionic character on the Li-O bond. Nonetheless, with a yield of 3.86 at $E_p = 0.6$ keV for sample O1 as shown in figure 2.3.7.3, Li-O surface termination would be a good implementation in electron multiplying devices as it can amplify up to four times as much as the incoming current.

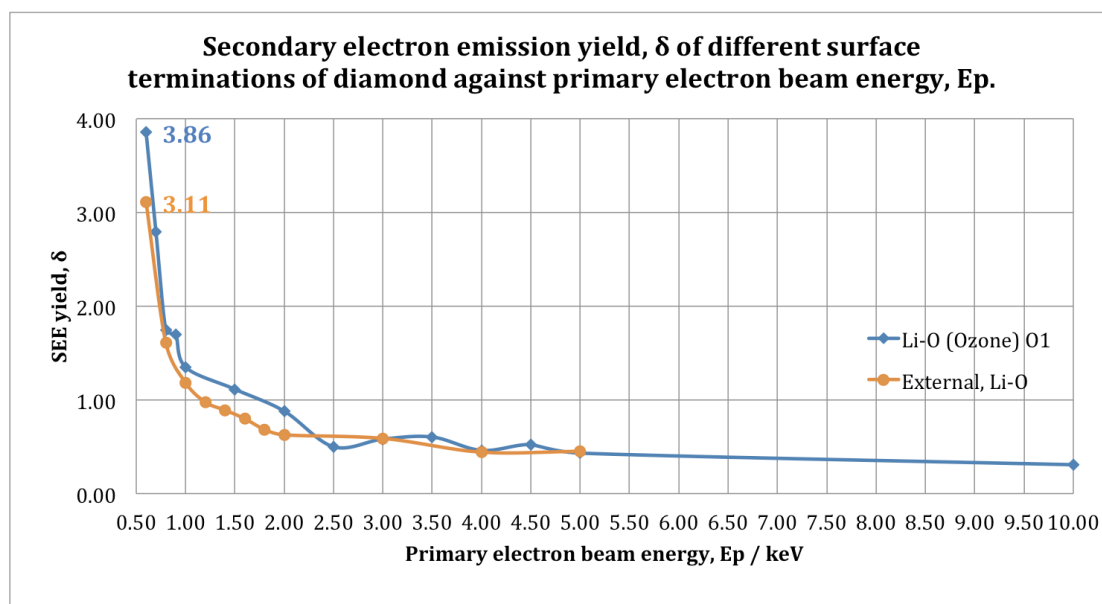


Figure 2.3.7.3: Li-O-terminated samples were shown. Blue curve was the sample prepared in this experiment while orange curve was the sample obtained externally.

The general pattern of the yield curve as a function of E_p for all samples showed high yield at low E_p and low yield at higher E_p values. Due to the limitation of the set-up, the SEE yield graphs in this study cannot confirm that the maximum SEE yield, δ_{\max} occurred at 0.6 keV. Higher yield occurring at low primary energy can be supported by the fact that primary electrons having low energy generally correlate to a low penetration depth. As a consequence of having a small penetration depth, secondary electrons will be emitted near the surface resulting in a higher yield. This is because, in theory, the penetration depth of the primary beam has to be comparable to the escape depth of secondary electrons to maximize the probability of emission from a surface. By law, low energy electrons may have inadequate energy to excite electrons, however due to the presence of NEA on the surface, electrons that occupy conduction band were spontaneously emitted. In contrary to the low yield, at higher E_p , high primary energy electrons have high velocity^[43] so they tend to penetrate deeper into the bulk of the diamond. Even though more secondary electrons may be generated in the bulk, internal secondary electrons lose energy during their transmission to the surface by scattering mechanism. Electron-impurity scattering reduced the energy of internal secondary electrons so by the time they reach the surface; they no longer have sufficient energy to overcome the barrier to emission. Since the samples used were all highly B-doped, this would mean internal secondary electrons generated in the bulk have high frequency of collisions with boron dopants incorporated in the diamond lattice. Simply put, at high primary energy, even so more secondary electrons might be excited, there were only a small portion of secondary electrons that have an optimum escape depth to overcome the vacuum barrier,^[48] while the rest of the secondary electrons in the bulk have their escape depth reduced as a result of collision in the bulk.

The possibility of getting a low SEE yield from a H-terminated sample in this experiment compared to the past studies could be due to the residual dangling

bonds on the surface that were not attached with hydrogen during the treatment of sample in the MWCVD or the desorption of hydrogen upon electron bombardment. The SEM image of H-terminated sample on figure 2.3.6.5 showed an uneven brightness on the surface indicating that the surface was not evenly hydrogen terminated. Dangling bonds are capable of trapping secondary electrons at a considerably low amount i.e. 1 electron trapped per 10 000 conventional unit cells on the surface ^[49]. It should be emphasized that the yield values from this experiment can not be compared to literature values as there are other factors that needed to be taken into account such as the method used to measure SEE yield, difference in samples; type of facets, crystal type and also boron dopant concentration, are among other things that need to be considered before the yields can be compared. It would be sufficient to compare the yield values of the different surface terminations in this project, as they were prepared on the diamond samples that have similar specifications bought in from the supplier.

The surface roughness could also indirectly caused a reduction in yield since the rough side of the samples was used whereas most studies have used the smooth side of the diamond sample. Roughness of a surface can decrease the NEA surface by building up charges on the surface that can prevent the emission of secondary electrons.

2.4 Conclusion

The contrast of brightness on the SEM image of the samples proved the different SEE properties generated by different surface terminations. H-terminated sample was significantly brighter than O-terminated, Li-O-terminated and LiF-O-terminated samples. Since the brightness between O-terminated, Li-O-terminated and LiF-O-terminated were not distinct, SEE yield measurement showed that at $E_p=0.6$ keV, H-terminated undoubtedly had the highest yield of $\delta=5.88$ followed by Li-O-terminated $\delta = 3.86$, O-terminated $\delta=1.57$ and unexpectedly LiF-O-terminated sample with the lowest yield of $\delta=1.48$. This low yield can only be illustrated by the coordination of LiF on the O-terminated sample. Though the exact coordination could not be determined from this study but a possible assumption was that LiF was not bonded to O-terminated sample to form a dipole layer on the surface. However result from the contact angle showed LiF-O-terminated having the lowest contact angle of $\theta=12.5^\circ$, revealing the most hydrophilic sample. LiF-O-terminated sample can be interpreted as possessing a negative top layer on the surface. But then again, the thick layer of LiF deposited on the O-terminated sample might have impeded the emission of secondary electrons.

Whilst the surface characterization test confirmed the formation of different surface terminations on the diamond, SEM images of the samples showed inconsistent brightness indicating non-homogenous terminations due to the presence of high level of roughness on the surface. Previously mentioned non-uniform surface coverage may affect the emission character on the surface causing a difference in yield from one specific point to another, hence explaining why the yields of similar surface terminations were not analogous.

Since the boron concentrations of all the samples were the same and only surface terminations have been done to the samples, therefore, the different emission characters came from the surface treatment and not the bulk properties. It can be concluded that secondary electron emission was dependent on the surface morphology.

2.5 Future work

As a further study, LiF-O-terminated sample can be treated for X-ray activation under the XPS to activate the excess layer of approximately 30Å deposited on the surface. The yield performance of the unactivated, excess LiF film that has been done in this study can then be compared to the yield behavior after the activation process. If the yield of LiF-O-terminated sample would be improved after the X-ray initiation method, this may give an indication that the LiF has been coordinated to the O-terminated sample. Hopefully it can aid in the explanation to why the inactive LiF-O-termination in this study did not result in a high SEE yield.

Another method to define exactly how LiF was bonded onto the diamond surface could be done with the help of a fluorine-terminated sample as a control. It would have been helpful to have fluorine directly terminated to the carbon of the diamond surface so the bonding on the surface could be characterized properly. The F-terminated diamond would then be compared to the LiF-O terminated and O-terminated sample, to see whether or not the fluorine atom has replaced the oxygen atom on the diamond surface. However, modifying the surface of the diamond to attach fluorine directly onto the carbon atom of diamond would need activated radical species to react, which not only require special equipment, but the techniques involved were also harsh and corrosive. Previous studies have tried activating the H-terminated diamond covered in fluorine-containing liquid by illuminating the sample with UV radiation. However the energy of the UV light of ~ 254nm was only sufficient to induce the formation of C-C bond and not C-F bond. [37] If an organic layer of fluorocarbon compound could be fabricated on H-terminated diamond, irradiating the layer with X-ray source from an XPS could potentially activate fluorine radical to abstract the diamond surface. As a further work, it would be interesting to find a suitable organic fluorine-containing compound.

With the support of further analysis such as Auger electron spectroscopy, the exact thickness of LiF can be determined. And for the actual coordination of LiF-O-termination, XPS would be a non-destructive analysis technique that can be used to study the composition and chemical bonds formed on the surface of the diamond.

2.6 Appendices

2.6.1 EDX data

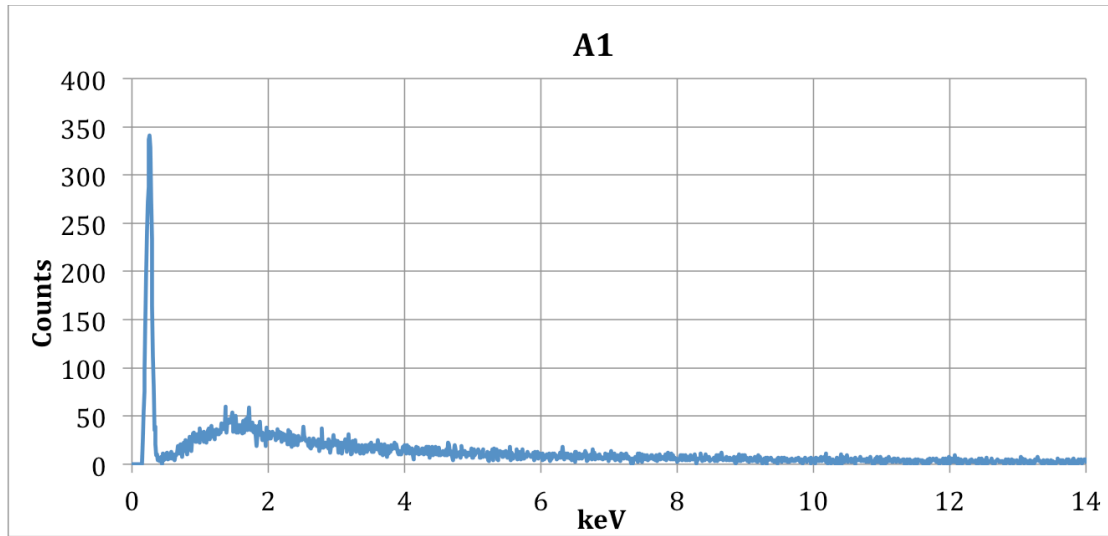


Figure 2.6.1.1: EDX spectrum of sample A1

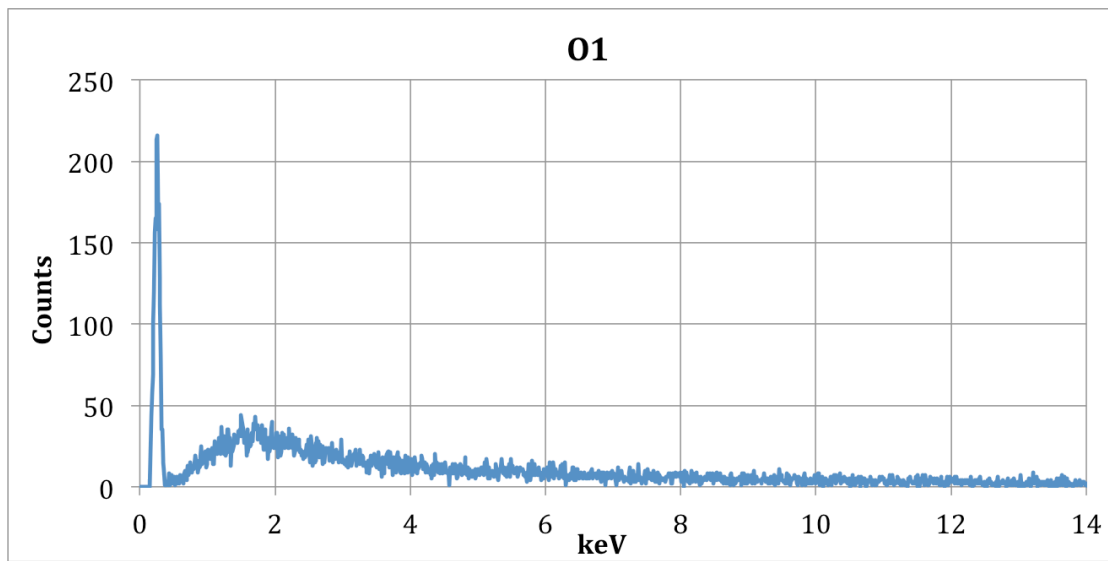


Figure 2.6.1.2: EDX spectrum of sample O1

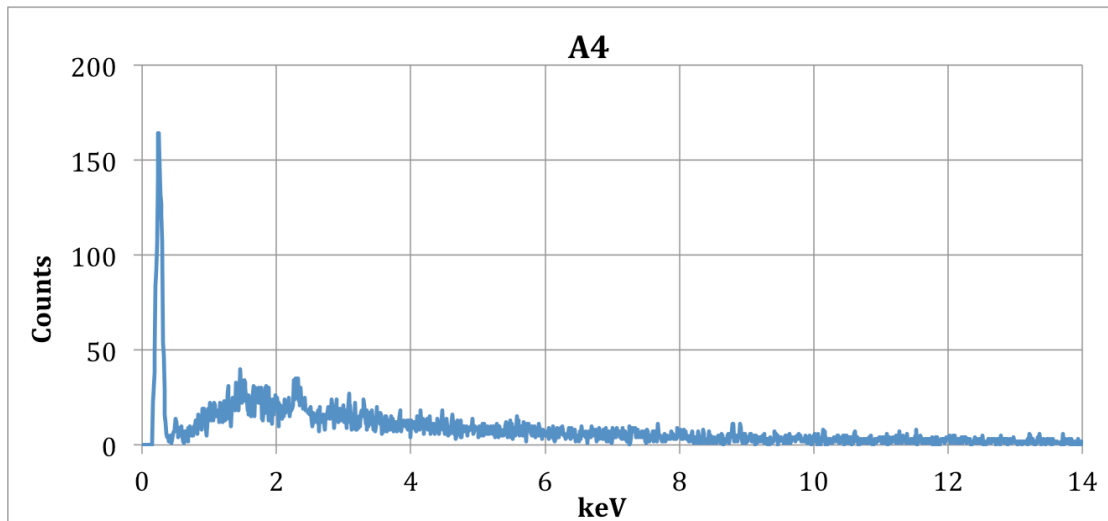


Figure 2.6.1.3: EDX spectrum of sample A4

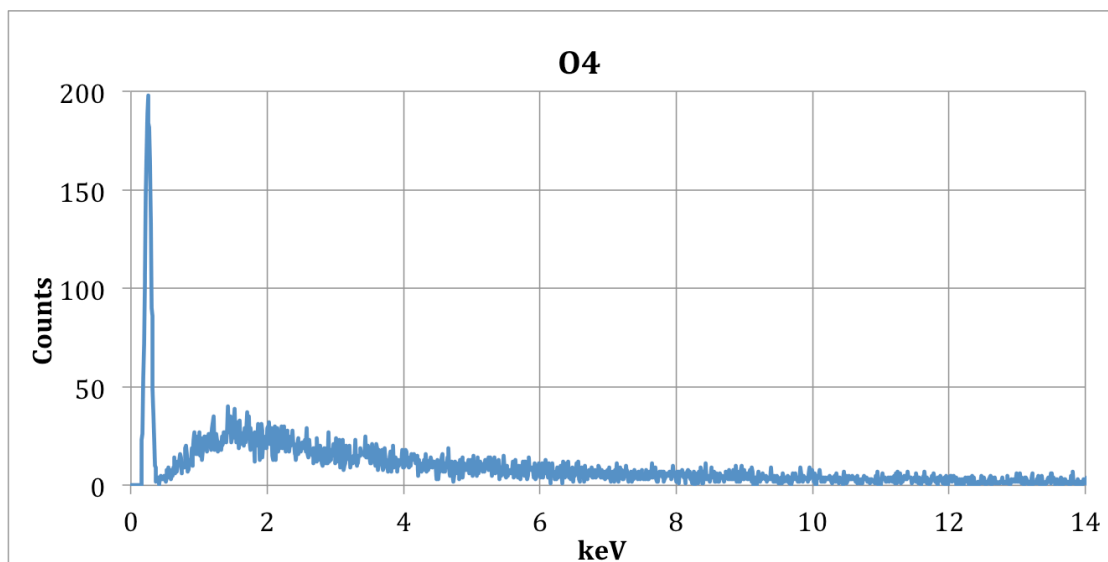


Figure 2.6.1.4: EDX spectrum of sample O4

2.6.2 Contact angle data



Figure 2.6.2.1: Drop profile of Test sample

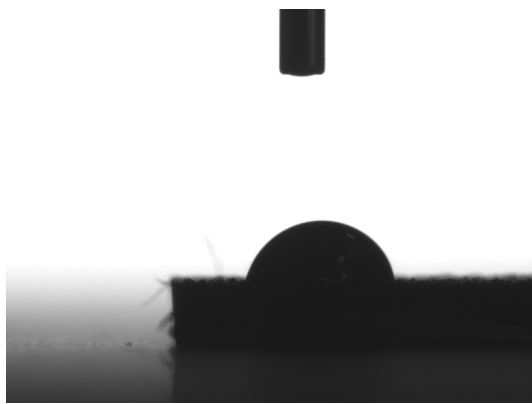


Figure 2.6.2.2: Sample A5 with O-termination



Figure 2.6.2.3: Sample O5 with O-termination

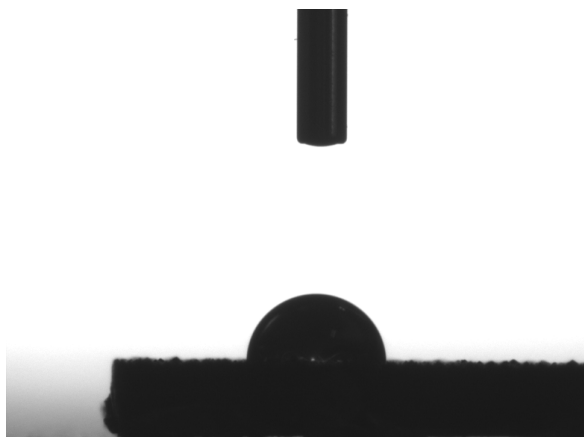


Figure 2.6.2.4: Sample A1 with Li-O-termination

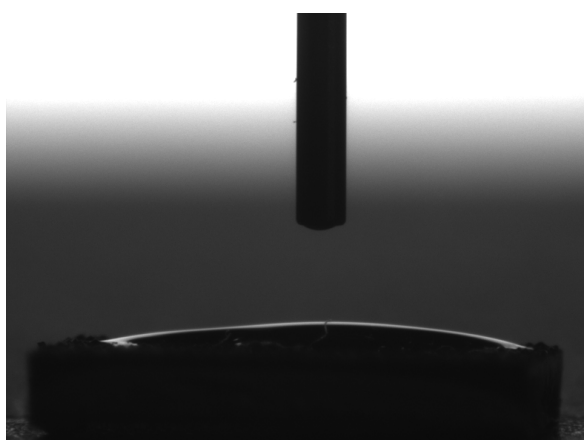


Figure 2.6.2.5: Sample A2 with LiF-O-termination

2.6.3 SEM data

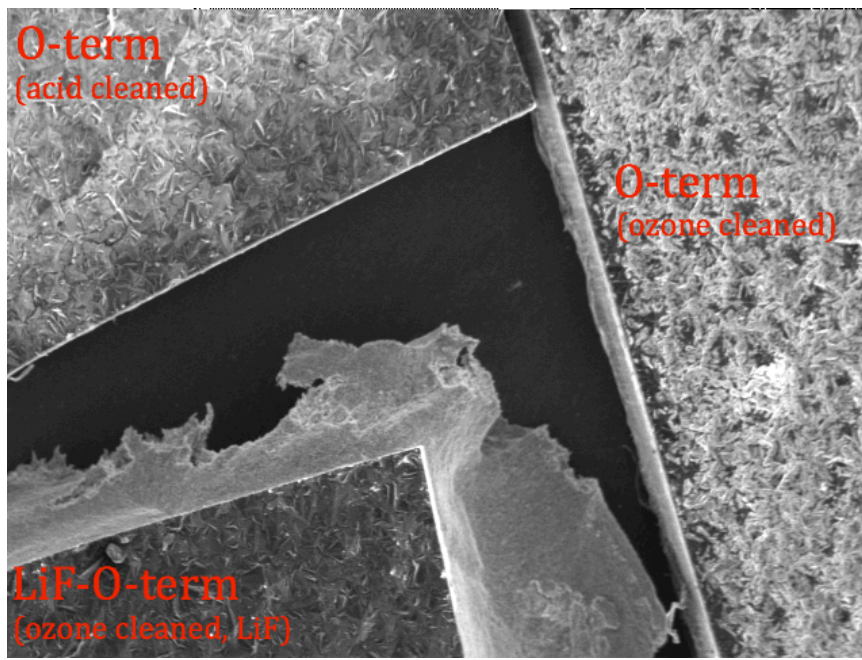


Figure 2.6.3: Brightness comparison between three samples.

2.7 References

- [1] E. Anastassakis, A. Cantarero and M. Cardona, *Phys. Rev. B*, 1990, 41, 7529-7535.
- [2] G. Davies and Institution of Electrical Engineers, *Properties and growth of diamond*, Institution of Electrical Engineers (INSPEC), London, 1994.
- [3] J. S. Lapington, P.W. May, N.A Fox, J. Howorth, JA. Milnes, *Laser Focus World*, September 2008
- [4] A. Shih, J. Yater, P. Pehrsson, J. Butler, C. Hor, and R. Abrams, *J. Appl. Phys*, 1997, 82, 1860-1866
- [5] J. E. Field, *The properties of natural and synthetic diamond*, Ed. Academic Press, 1992
- [6] K. Fabisiak and E. Staryga, *Journal of Achievements in Materials and Manufacturing Engineering*, 2009, 37(2), 264-269
- [7] G. Pastor-Moreno, PhD Thesis, University of Bristol, 2002
- [8] L. Diederich, O.M. Küttel, P. Ruffieux, T. Pillo, P. Aebi, L. Schlapbach, *Surf. Sci.*, 1998, 417, 41-52
- [9] L. Diederich, O.M. Kuttel, P. Aebi and L. Schlapbach, *Surf. Sci.*, 1998, 418, 219-239
- [10] T. L. Martin, PhD Thesis, University of Bristol, 2011
- [11] G. S. Painter, D. E. Ellis, A. R. Lubinsky, *Phys. Rev. B*, 1971, 4(10), 3610-3622
- [12] J. E. Yater, A. Shih, and R. Abrams, *J. Vac. Sci. Technol. A*, 1998, 16, 913
- [13] R. V. D. Bogaerde, Bsc. Undergraduate Thesis, University of Bristol, 2012
- [14] W. Simon, BSc Undergraduate Thesis, University of Bristol, 2012
- [15] A. Shih, J. Yater, C. Hor and R. Abrams, *Appl. Surf. Sci.*, 1997, 111, 251-258
- [16] J. B. Cui, J. Ristein, and L. Ley, *Phys. Rev. Lett.*, 1998, 81(2), 429
- [17] C. Bandis and B.B. Pate, *Phys. Rev. Lett.*, 1995, 74(5), 777-780
- [18] I. L. Krainsky, V. M. Asnin, G. T. Mearini, and J. A. Dayton, Jr., *Phys. Rev. B*, 1996, 53(12), R7650
- [19] J. Robertson, *Diamond Relat. Mater.*, 1996, 5, 797-801
- [20] P. G. Lurie and J. M. Wilson, *Surf. Sci.*, 1977, 65, 476-498
- [21] J. B. Miller and G. R. Brandes, *J. Appl. Phys.*, 1997, 82, 4538
- [22] V. M. Asnin and I. L. Krainsky, 9th International Vacuum Microelectronics Conference, St. Petersburg, 1996, 354-357

- [23] C.D. Clark and C.B Dickerson, *Phil. Trans. R. Soc. Lond. A.*, 1993, 342, 253-260
- [24] M. N. R. Ashfold, P. W. May, C. A. Rego and N. M. Everitt, *Chem. Soc. Rev.*, 1994, 23, 31
- [25] J. E. Graebner, S. Jin, W. Kammiott, J. A. Herb and C. F. Gardinier, *Appl. Phys. Lett.*, 1992, 60, 1576
- [26] I.L. Krainsky, V.M. Asnin and J.A. Dayton Jr., *Appl. Surf Sci.*, 1997, 111, 265-269
- [27] M. W. Geis, J. C. Twichell, J. Macaulay, and K. Okano, *Appl. Phys. Lett.*, 1995, 67(9). 1328-1330
- [28] G. T. Mearini, I. L. Krainsky, J. A. Dayton, Jr., Y. Wang, C. A. Zorman, J. C. Angus, R. W. Hoffman, D. F. Anderson, *Appl. Phys. Lett.*, 1995, 66, 242
- [29] M. Rutter and J. Robertson , *Phys. Rev. B*, 1998, 57, 9241-9245.
- [30] J. v. D. Weide , Z. Zhang, P. Baumann, M. Wensell, J. Bernholc and R. Nemanich, *Phys. Rev. B*, 1994, 50(8)
- [31] F. Maier, J. Ristein and L. Ley, *Phys. Rev. B*, 2001, 64(16), 165411
- [32] K. M. O'Donnell, T. L. Martin, N. A. Fox and D. Cherns, *Phys. Rev. B.*, 2010, 82, 115303
- [33] G. T. Mearini, I. L. Krainsky, J. A. Dayton, Jr., C. Zorman, Y.Wang and A. Lamouri, *Diamond Films Technol.*, 1995, 5(6), 339-352
- [34] N. Fox, P. May, M. Ashfold, N. Allan and J. Lay, Diamond Surfaces for Energy Applications [Powerpoint], NSQI User Seminar, University of Bristol, 2011
- [35] G. P. Smestad, *Sol. Energ. Mat. Sol. C.*, 2004, 82, 227-240
- [36] D.M. Trucchi, E. Cappelli, N. Lisi, P. Ascarelli, *Diamond Relat. Mater.*, 2006, 15, 1980-1985
- [37] S. Szunerits and R. Boukherroub, *J. Solid State Electrochem.*, 2008, 12, 1205-1218
- [38] J.M. Garguilo, B.A. Davis, M. Buddie, F.A.M. Kóck and R.J. Nemanich, *Diamond Relat. Mater.*, 2004, 13, 595-599
- [39] Y.M. Wang, K.W. Wong, S.T. Lee, M. Nishitani-Gamo, I. Sakaguchi, K.P. Loh and T. Ando, *Diamond Relat. Matter.*, 2000, 9, 1582-1590
- [40] D. R. Lide, *CRC Handbook of Chemistry and Physics.* , CRC Press, Boca Raton, FL, 73th ed., 1992/1993
- [41] J. van der Weide, Z. Zhang, P. K. Baumann, M. G. Wensell, J. Bernholc, and R. J. Nemanich, *Phys. Rev. B*, 50(8), 5803-5806
- [42] L. Ostrovskaya, V. Perevertailo, V. Ralchenkob A. Dementjev and O. Loginova, *Diamond Relat. Mater.*, 2002, 11, 845-850

- [43] Y. Kaibara, K. Sugata, M. Tachiki, H. Umezawa and H. Kawarada, *Diamond Relat. Mater.*, 2003, 12, 560-564
- [44] R. S. Sussmann, *CVD Diamond for Electronic Devices and Sensors*, John Wiley & Sons Ltd, Chippenham, Wiltshire, 2009, Section 18.3.1.2, 490
- [45] M.C. Salvadori, W.W.R. Araújo, F.S. Teixeira, M. Cattani, A. Pasquarelli, E.M. Oks and I.G. Brown, *Diamond Relat. Mater.*, 2010, 324-328
- [46] V. Konduru, MSci Thesis, Michigan Technological University, 2010
- [47] K.W. Wong, Y.M. Wang, S.T. Lee, R.W.M. Kwok, *Diamond Relat. Mater.*, 8, 1885-1890
- [48] J.J. Scholtz, D. Dijkkamp and R. W. A. Schmitz J.J. , *Philips J. Res.*, 1996, 50, 375-389
- [49] Q. Wu, PhD Thesis, Indiana University, 2008
- [50] F. P. Bundy, *J. Geophys. Res.*, 1980, 85, 6930-6936
- [51] M. Wieser, P. Wurz, R. J. Nemanich, and S. A. Fuselier , *J. Appl. Phys.*, 2005, 98, 34906
- [52] G. T. Mearini, I. L. Krainsky, J. A. Dayton, Y Wang, C. A. Zorman, J. C. Angus and R. W. Hoffman, 1994, *Appl. Phys. Lett.*, 65, 2702-2704
- [53] H.J. Hopman, J. Verhoeven , P.K. Bachmann, H. Wilson, R. Kroon, *Diamond Relat. Mater.*, 1999, 8, 1033-1038
- [54] M. T. Edmonds, M. Wanke, A. Tadich, H. M. Vulling, K. J. Rietwyk, P. L. Sharp, C. B. Stark, Y. Smets, A. Schenk, Q. H. Wu, L. Ley and C. I. Pakes, *J. Chem. Phys.*, 2012, 136, 124701
- [55] C. Bandis and B.B. Pate, *Phys. Rev. B.*, 1995, 52(16), 12 056
- [56] A. Hoffman, M. Folman and S. Prawer, *Phys. Rev. B*, 1991, 44(9), 4640
- [57] B. Marczewska, P. Bilski, P. Olko, M. Nesladek, M. Rębisz and M. J. Guerrero, *Radiat. Prot. Dosim.*, 2006, 1-4
- [58] J.B Johnson, *Phys Rev.*, 1953, 92, 843
- [59] K. J. Rietwyk, M. Wanke, H. M. Vulling, M. T. Edmonds, P. L. Sharp, Y. Smets, Q.-H. Wu, A. Tadich, S. Rubanov, P. J. Moriarty, L. Ley and C. I. Pakes, *Phys. Rev. B*, 2011, 84, 035404
- [60] Kazuhiro Kanda, Noriko Yamada, Kumiko Yokota, Masahito Tagawa, Masahito Niibe, Makoto Okada, Yuichi Haruyama and Shinji Matsui, *Diamond Relat. Mater.*, 2011, 703-706,
- [70] S. Hadenfeldt and C. Benndorf, *Surf. Sci.*, 1998, 402-404, 227-231
- [71] A. P. Kharitonov and L. N. Kharitonova, *Pure Appl. Chem.*, 2009, 81(3), 451-471

- [72] C. S. Kim, R. C. Mowrey, J. E. Butler, and J. N. Russell, Jr., *J. Phys. Chem. B*, 1998, 102, 9290-9296
- [73] V. Baglin, J. Bojko, O. Gröbner, B. Henrist, N. Hilleret, C. Scheuerlein and M. Taborelli, *Proceedings of EPAC 2000*, Vienna, Austria, 217-221
- [74] N. D. Zamoski, P. Kumar, C. Watts, T. Svimonishvili, M. Gilmore, E. Schamiloglu, J. A. Gaudet, *IEEE Trans. Plasma Sci.*, 2006, 34(3), 642-651
- [75] C. E. Nebel, N. Yang and H. Uetsuka, *Surf. Sci.*, 2008, 603, L5-L8
- [76] H. Touhara and F. Okino, *Carbon*, 2000, 38, 241-267
- [77] A. N. D'yachenko and R. I. Kraidenko, *Russ. J. Appl. Chem.*, 2008, 81(6), 952-955
- [78] D. E. Patterson, PhD Thesis, Rice University, 1989
- [79] D. W. Harwood, E. R. Taylor, R. Moore and D. Payne, *J. Non Cryst. Solid*, 2003, 332, 190-198
- [80] T. Easwarakhanthan, D. Beyssen, L. Le Brizoual, and J. Bougdira, *J. Vac. Sci. Technol. A*, 2006, 24, 1036-1043
- [81] A. Kraft, *Int. J. Electrochem. Sci.*, 2007, 2, 355-385
- [82] Y. L. Zhong and K. P. Loh, *Chem. Asian. J.*, 2010, 5, 1532-1540
- [83] S.J. Henley, M.N.R. Ashfold, S.R.J. Pearce, *Appl. Surf. Sci.*, 2003, 217, 68-77
- [84] K. Larsson, *Diamond Science and Technology*, Frontiers in Science and Technology, 2002, 1, 63-64
- [85] J.E. Huheey, *Inorganic Chemistry, Principles of Structure and Reactivity*, Harper & Row, New York, 1983, A31